



저작자표시-비영리-변경금지 2.0 대한민국

이용자는 아래의 조건을 따르는 경우에 한하여 자유롭게

- 이 저작물을 복제, 배포, 전송, 전시, 공연 및 방송할 수 있습니다.

다음과 같은 조건을 따라야 합니다:



저작자표시. 귀하는 원저작자를 표시하여야 합니다.



비영리. 귀하는 이 저작물을 영리 목적으로 이용할 수 없습니다.



변경금지. 귀하는 이 저작물을 개작, 변형 또는 가공할 수 없습니다.

- 귀하는, 이 저작물의 재이용이나 배포의 경우, 이 저작물에 적용된 이용허락조건을 명확하게 나타내어야 합니다.
- 저작권자로부터 별도의 허가를 받으면 이러한 조건들은 적용되지 않습니다.

저작권법에 따른 이용자의 권리는 위의 내용에 의하여 영향을 받지 않습니다.

이것은 [이용허락규약\(Legal Code\)](#)을 이해하기 쉽게 요약한 것입니다.

[Disclaimer](#)

**ENHANCING PLC-WIFI NETWORK CONNECTIVITY
AND RADIO ENVIRONMENT MAP CONSTRUCTION
THROUGH FEDERATED LEARNING**

DISSERTATION

for the Degree of

MASTER OF PHILOSOPHY
(Electrical Engineering)

SHAFI ULLAH KHAN

FEBRUARY 2024

**Enhancing PLC-WiFi Network Connectivity and Radio
Environment Map Construction Through Federated Learning**

DISSERTATION

Submitted in Partial Fulfillment
of the Requirements for the
Degree of

MASTER OF PHILOSOPHY
(Electrical Engineering)

at the

UNIVERSITY OF ULSAN

by

Shafi Ullah Khan

February 2024


Publication No.

©2024 - Shafi Ullah Khan

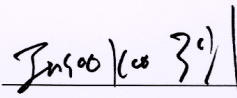
All rights reserved.

**Enhancing PLC-WiFi Network Connectivity and Radio
Environment Map Construction Through Federated Learning**


Approved by Supervisory Committee:



Prof. Sungoh Kwon , Chair



Prof. In-Soo Koo, Supervisor



Prof. Hee-Youl Kwak

Department of Electrical Electronics and Computer Engineering,

University of Ulsan, South Korea

November, 2023

VITA

Shafi Ullah Khan received his Bachelor of Engineering (B.E.) in Electrical Engineering from the University of Science and Technology Peshawar, Pakistan, in 2020. In September 2021, he started pursuing his Master's degree in Electrical Engineering, under the supervision of Professor In-Soo Koo, at the school of Electrical Engineering, University of Ulsan (UOU), South Korea. His research interests include wireless communication, power line communication, machine learning, federated learning and internet of things (IoT).

Dedicated to my parents, whose
unwavering love and belief in
me have been the guiding
stars of my journey.

ACKNOWLEDGMENTS

First and foremost, I am profoundly grateful to Almighty Allah for His countless blessings upon me. Without His mercy, I would not have been able to complete this degree.

Every achievement in my life is owed to my pillars of strength, my father Mr. Aziz Ullah, and my mother Sajida Bibi. Their unwavering guidance and encouragement from my early school days have been instrumental in all that I have accomplished.

I am also deeply thankful to all my siblings for their prayers, love, and care. A special mention goes to my elder brother, Mr Zia Ullah who has always been available whenever I needed his guidance and support.

My heartfelt gratitude goes to my supervisor, Professor In-Soo Koo. Being part of his research group was a privilege. His invaluable guidance, consistent encouragement, and kindness have been pivotal throughout my Master's degree journey. Words fall short in expressing my true appreciation.

I wish to convey my sincere appreciation to Dr. Sana Ullah Jan. His enthusiasm and unwavering support throughout this journey were indispensable. This dissertation would not have come to fruition without his guidance.

I would also like to extend my thanks to the other members of my Master's supervisory committee, Prof. Sungoh Kwon and Prof. Hee-Youl Kwak, for their valuable feedback. I'm grateful to all the members of the Multimedia Communication Systems Laboratory (MCSL) for their camaraderie over the last two years. A special thanks to MD Nazmul Hasan and Hafiza Iqra Hameed for their unwavering support during challenging times.

Lastly, my appreciation goes to the Pakistani community at UoU for their love, respect, and consistent support.

Shafi Ullah Khan

Ulsan, South Korea, February - 2024.

ABSTRACT

Enhancing PLC-WiFi Network Connectivity and Radio Environment Map Construction Through Federated Learning

by

Shafi Ullah Khan

Supervisor: Professor In-Soo Koo

Submitted in Partial Fulfillment of the Requirements for the Degree of
Master of Philosophy (Electrical Engineering)

February 2024

In today's rapidly evolving industrial landscape, the intersection of technology and operational processes is increasingly evident. As industries transition into the digital era, there's a pressing need for powerful, efficient, and secure communication infrastructures. Central to this transformation is the deployment of hybrid broadband Power Line Communication (PLC) and Wi-Fi networks, adept at catering to the diverse demands of modern digitalized industries. These networks, with their unique blend of technologies, offer promising solutions for enhancing communications within challenging indoor industrial spaces. However, determining the coverage efficiency of such networks remains a significant challenge. In addressing this challenge, the application of radio environment mapping (REM) emerges as a critical tool. REM provides quantitative metrics and graphical visualizations to assess network coverage and performance across diverse industrial infrastructures.

First, a real industrial network has been made in the University of Ulsan using PLC and Wi-Fi hybrid network. We explore potential applications of a hybrid broadband

Power Line Communication (PLC) and Wi-Fi in an indoor hospital scenario. As, modern hospitals urgently require a mobile, high-capacity, secure, and cost-effective communication infrastructure. It utilizes the existing power line cables and Wi-Fi Plug-and-Play devices for indoor broadband communication. Broadband Power Line (BPL) adaptors with Wi-Fi outputs are used to build an access network in hospitals, particularly in areas where the wireless router signal is poor. The Tenda PH10 AV1000 ACWI-FI POWER LINE ADAPTER is a set of BPL adapters that offer operational bandwidth of up to 1000Mbps. These adapters are based on the HomePlug AV2 protocol and can provide a data rate up to 200 Mbps on the Physical Layer. An experiment using the PLC Wi-Fi kit is carried out to show that a Wi-Fi and PLC hybrid network is the best candidate to provide wide range of practical applications in a hospital including, but not limited to, telemedicine, electronic medical records, early-stage disease diagnosis, health management, real-time monitoring, and remote surgeries.

Furthermore, coverage prediction stands essential to optimizing radio networks, thereby enhancing user experience. A number of path loss models and advanced machine learning algorithms have been developed with high prediction performance. However, these models conventionally operate within a centralized learning paradigm. Conversely, in this article, we proposed a novel decentralized approach based on a federated learning long short-term memory (LSTM) model to predict accurate network coverage in indoor settings. The proposed FedLSTM is a method that lets multiple users, or clients, train the model without sharing their personal data directly with a central server. In an experimental setup, we utilized real data collected from numerous clients moving along different paths. The FedLSTM model is evaluated in terms of root mean square error (RMSE), mean absolute error (MAE), and R^2 . Moreover, compared with a centralized counterpart, FedLSTM shows a slight rise in RMSE from 2.4 dBm to 2.5 dBm and an increase in MAE from 1.7 dBm

to 1.9 dBm. In addition, we evaluate the proposed FedLSTM considering variations in the number of participating clients and in the number of local training epochs. Results show that even devices with limited computational power can meaningfully contribute to training the federated model, with fewer epochs achieving competitive results. Graphic analyses of the radio environment maps (REMs) drawn from both FedLSTM and the centralized LSTM highlight their similarities. However, FedLSTM provides data privacy for clients while reducing communications overhead and server strain.

Contents

Vita	v
Dedication	vi
Acknowledgments	vii
Abstract	viii
Table of Contents	xi
List of Figures	xiii
List of Tables	xv
Nomenclature	xvi
1 Introduction	1
1.1 Motivation	1
1.2 Objective	5
1.3 Contribution and thesis outline	6
2 Efficient Indoor Industrial Communication Architecture using hybrid Wi-Fi and PLC network	8
2.1 Introduction	8
2.2 Network Structure	11
2.3 Performance Analysis of The Hybrid Network of Wi-Fi and PLC	15
2.3.1 Throughput Measurement	17
2.3.2 Effect of Load on Tenda PA7 Powerline Extender	19
2.3.3 Signal Strength Analysis	21
2.4 Applications and features of the hybrid system	22
2.4.1 Features	22
2.4.2 Possible Applications	24
2.5 Conclusion	25
3 Radio Environment Map Construction based on Privacy-centric Federated Learning	27
3.1 Introduction	27
3.2 Related Work	30
3.3 Data Collection and Preprocessing	34
3.3.1 Emesent Hovermap	34

3.3.2	SLAM Distance Measurement via LiDAR	36
3.3.3	RSSI Value Measurement	37
3.4	System Model	39
3.4.1	Federated Learning	40
3.4.2	FedLSTM Archeticture	41
3.4.3	REM Construction	43
3.4.4	Model Evaluation	46
3.5	Numerical Results	49
3.5.1	Comparison with a Centralized LSTM Network	50
3.5.2	Impact of the Number of Clients on Global Convergence	51
3.5.3	Contribution of Local Model Epochs to Global Convergence	56
3.6	Graphical Results	60
3.7	Conclusion	64
4	Summary of contributions and future works	66
4.1	Introduction	66
4.2	Summary of Contributions	68
4.3	Future Direction	70
	Publications	72
	Bibliography	74

List of Figures

1.1	Role of REM in cognitive radio	4
2.1	Tenda PH10 AV1000 AC Wi-Fi Powerline Kit	12
2.2	Industrial network design	13
2.3	Broadcom BCM47189B0 chip	14
2.4	Laboratory system setup for different lengths	15
2.5	Measurement Results	16
2.6	Startrinity CST home Page	17
2.7	System configuration	18
2.8	Location point within industrial network	18
2.9	Throughput variation with length	19
2.10	1400-Watt load connection	20
2.11	Performance of Tenda P10 with and without load	21
2.12	Signal strength analysis at different distances	22
3.1	EMESENT Hovermap	34
3.2	EMESENT Hovermap Rear View	36
3.3	Cloudmap of room 7-611	37
3.4	Raspberry Pi mounted on EMESENT Hovermap	38
3.5	Federated learning overview	40
3.6	REM Construction.	45
3.7	Fine-tuning the FedLSTM network for REM construction.	47
3.8	Performance Comparison of centralized and federated LSTM networks	51
3.9	R^2 variations from the number of clients	52
3.10	RMSE variations from the number of clients	53
3.11	MAE variations from the number of clients	54
3.12	Relative error based on the number of clients	55
3.13	MAPE variations based on the number of clients	56
3.14	RMSE variations from the local number of epochs	58
3.15	R^2 score variations based on the number of local epochs	59
3.16	Variations in relative error based on the number of local epochs	60
3.17	Variations in MAPE based on the number of local epochs	61
3.18	Variations in MAE based on the number of local epochs	62

3.19 (a) Corridor layout, (b) REM from the centralized LSTM model, and (c) REM from FedLSTM	63
3.20 (a) Room layout, (b) REM from the centralized LSTM model, and (c) REM from FedLSTM	64

List of Tables

3.1 Architecture of the LSTM Network 44

Nomenclature

Notation Description

AI	Artificial Intelligence
Adam	Adaptive Moment Estimation - a popular optimization algorithm
ANN	Artificial Neural Network
AP	Access Point
BB	Broad Band
BLP	Broad Band Power Line
BPS	Bits Per Second
FL	Federated Learning
IoT	Internet of things
K-NN	K- Nearest Neighbors
LAN	Local Area Network
LSTM	Long Short Term Memory
LTE	Long term evolution
MAC	Media Access Control
MIMO	Multiple-input multiple-output
ML	Machine Learning
NB	Narrow Band
PLC	Power Line Communication
QoS	Quality of Service
REM	Radio Environment Map
RF	Random Forest
SLAM	Simultaneous Localization And Mapping
SVM	Support Vector Machine
Wi-Fi	International Energy Agency
WLAN	Wireless Local Area Network
XGBoost	Extreme Gradient Boosting

Chapter 1

Introduction

1.1 Motivation

The 4.0 Industrial Revolution, characterized by the integration of the physical, digital, and biological systems, has placed the Internet at its core. Not only does it drive e-commerce, online education, telemedicine, e-banking, and other online transactions, but it is also a pivotal element in realizing Industry 4.0's vision of smart factories and interconnected devices. These modern industrial settings are increasingly reliant on rapid and reliable internet connections for efficient operations and real-time decision-making. The ever-expanding reach and utility of the Internet can be attributed to breakthroughs in technology, allowing for swift and seamless information exchange. Data from the International Telecommunication Union indicates that by 2020, about 51% of the global population is using the internet [1]. However, effective digital services require a strong communication network with mobile access, efficient data distribution, and fast data transfer speeds. To support digital data demands, networks need consistent throughput and optimal Quality of Service (QoS). Given this shift to digital, both public and private sectors are adopting advanced communication technologies. Recent advances, including developments in Local

Area Networks (LANs), Radio Frequency (RF), ZigBee, and Wide Area Networks (WANs), are driving this transition, especially in real-time applications [2].

Among them, wireless technologies have become increasingly popular in various fields, including e-commerce, online education, telemedicine, and e-banking applications. However, these technologies present several challenges related to signal dispersion and coverage range, especially when used across large regions [3,4]. For instance, Radio Frequency (RF) and Bluetooth-based devices face limitations when operating in areas with concrete walls and other obstructions [5,6]. Additionally, Ethernet-based systems may lack flexibility and may require expensive setup processes, particularly in buildings with multiple stories. To overcome these challenges, it is necessary to develop and integrate different technologies to build a hybrid network that combines the most used wireless technology with wired technology, resulting in a cost-effective and flexible solution. A hybrid network offers benefits such as improved coverage and reliability, increased bandwidth, and the ability to transmit large amounts of data even over a long distance. By integrating wired and wireless technologies, a hybrid network can overcome the limitations of each technology and leverage their respective strengths. The implementation of a hybrid network requires careful planning and design to ensure that it meets the specific requirements of the intended application. This involves selecting appropriate network components, such as routers, switches, Wi-Fi relays, and access points, and configuring them to work together seamlessly. Furthermore, it is essential to consider factors such as security, scalability, and manageability when designing a hybrid network.

Power line communication (PLC) has been extensively used to develop broadband networks with high data transmission rates based on power grids [7]. The PLC technology is designed to achieve burst data speeds of up to 20 Mbit/s over power-line connections, making it suitable for in-building multimedia applications. The superimposition of high-frequency

signals on the low-frequency power line signals enables communication over the power line network. The data rate of PLC technology has reached up to 200Mbps on the physical layer, which is higher than its theoretical value. This high data rate, like Wi-Fi and domestic Ethernet, makes it suitable for various applications, such as high-definition video streaming, video conferencing, online gaming, and cloud computing. One of the primary benefits of employing PLC networks is the ability to reuse the existing wired electrical network to offer communication capabilities, making it cost-effective for broadband communication applications. Moreover, the PLC technology offers a robust and reliable communication infrastructure without the need for new cabling, thus avoiding wireless propagation issues. Hence, the smart grid remains one of the most appealing uses of PLC technology, and research in this field is extensive. In addition to smart grid applications, PLC technology has also proven its effectiveness in smart city [8], in-home automation [9], and telemetry [10] applications, where new cabling is not required, and wireless propagation issues are avoided. Furthermore, PLC-based plug-and-play extenders are gaining popularity in the market due to their easy installation and connectivity [11]. Therefore, PLC technology has become a promising solution for both broadband (BB) applications, such as interactive multimedia home with video conferencing, and narrowband (NB) communication, such as IoT smart house. The integration of wired and wireless technologies in a hybrid network can address the limitations of each technology while leveraging their strengths. However, the use of wireless technology in the hybrid network can also lead to signal dispersion issues, resulting in shadow areas where signal strength is weakened or absent due to obstructions such as walls, floors, or other physical barriers. These shadow areas can negatively impact network performance and security, leading to decreased productivity and efficiency.

Recognizing the conditions in the operating environment is crucial for optimizing resource use in different adaptive systems. In the Fourth Industrial Revolution, this is

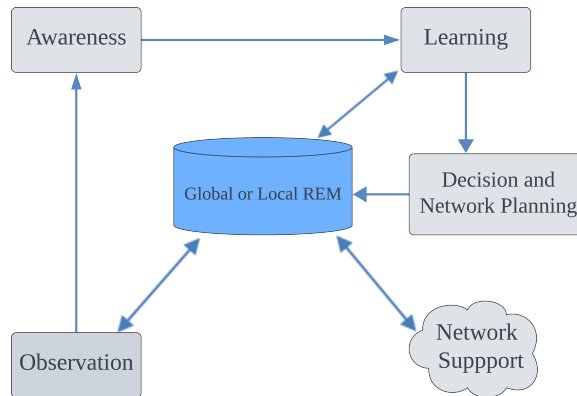


Figure 1.1: Role of REM in cognitive radio

highlighted by the introduction of tools like artificial intelligence, big data analytics, the Internet of Things (IoT), and robotics in modern manufacturing. These tools help automate and monitor processes in real-time, ensuring timely adjustments [12].

Wireless communication is fundamental to smart factories, enabling real-time monitoring and control of production processes. However, the rise in wireless devices brings interference issues, especially within the industrial, scientific, and medical (ISM) band [13]. Indoor setups can weaken signals, creating radio 'blind spots.' Thus, evaluating radio communication's coverage becomes important. To tackle this, Radio Environment Map (REM) has been explored. Building the REM involves collecting actual data from the target area. This data helps in understanding the wireless environment's patterns and is visualized similar to a temperature map. REM provides detailed data on radio conditions in defined areas, helping network managers identify coverage gaps and high-demand areas [14].

REM plays a very important role in cognitive cycle of cognitive radios, as shown in Figure 1.1. Primarily, REM offers an comprehensive awareness of the prevailing radio environment. By tracking signal dispersion, it provides critical insights into how signals spread or attenuate across different regions. Furthermore, its ability to continually learn from the environment ensures that it adapts to evolving conditions. This continuous learning,

in turn, equips network planners with the data necessary for informed decision-making, facilitating both strategic network expansion and dynamic adaptation. Additionally, REM plays an integral role in bolstering network support, enhancing overall system reliability and performance. Traditionally, REM is constructed following a centralized approach, wherein all device data is sent to a central server. This architecture not only raises concerns regarding user data confidentiality and security but also places a significant computational and communication burden on the central server, potentially compromising efficiency and scalability.

1.2 Objective

This thesis primarily focuses on improving the indoor connectivity within industrial networks and identifying network shadow areas. Initially, we developed a prototype of the industrial network integrating both PLC and Wi-Fi technologies, delving into the potential applications of this hybrid PLC-Wi-Fi setup for industrial scenarios.

Subsequently, our goal shifted to identifying the shadow areas within the wireless segment, aiming to enhance network coverage predictions for more efficient planning and user experience. In addressing this, we constructed an REM for the area of our interest. However, instead of the traditional approach, we incorporated federated learning techniques for predicting the coverage in indoor setting. This method not only prioritizes user data privacy but also optimizes communication efficiency. This approach prioritizes user data privacy, minimizes communication overhead, and alleviates central server load by transmitting only model weights rather than the exhaustive raw data.

1.3 Contribution and thesis outline

This dissertation investigates the potential applications of PLC-Wi-Fi hybrid networks specifically for industrial environments. It rigorously examines the key characteristics of the constructed industrial network, including its capacity, data integrity, transmission rate, and user privacy. Additionally, the construction of a REM for indoor settings, aimed at amplifying connectivity and enhancing user experience. A novel method to forecast received signal strength indicator (RSSI) values based on spatial coordinates within a decentralized framework is introduced. The efficacy of this decentralized method was assessed under various federated configurations and subsequently evaluated using error metrics. The rest of this thesis and its contribution chapters of this dissertation, detailing its contributions, are structured as follows:

- **Chapter 2:** Discusses the prevalent challenges in the e-health domain, proposing an avant-garde methodology to augment communication infrastructures within contemporary healthcare settings. Recognizing the urgent need for an advanced, mobile, high-capacity, secure, and economically feasible communication infrastructure in healthcare facilities, we delve into the potential of combining hybrid broadband Power Line Communication (PLC) and Wi-Fi for indoor hospital settings. Leveraging existing power line cables and plug-and-play Wi-Fi devices, we introduce the application of Broadband Power Line (BPL) adaptors with Wi-Fi capabilities, specifically targeting areas with weak wireless router signals. Our study prominently features the Tenda PH10 AV1000 ACWI-FI POWER LINE ADAPTER, a BPL adapter set promising an operational bandwidth reaching 1000Mbps. Operated by the HomePlug AV2 protocol, these adaptors are capable of delivering a data rate of up to 200 Mbps at the Physical Layer. Through experimental tests with the PLC Wi-Fi kit, we establish the robustness

and adaptability of the hybrid Wi-Fi and PLC network, proving its viability to support a vast spectrum of practical hospital applications. This includes telemedicine, electronic medical record systems, early disease detection, health management processes, instantaneous patient monitoring, and facilitating remote surgical procedures.

- **Chapter 3:** introduces the FedLSTM, a pioneering Long Short-Term Memory (LSTM) framework empowered by federated learning, specifically for indoor network coverage prediction. This offers a departure from traditional centralized learning schemes. Unique to our approach is its decentralized learning mechanism: the FedLSTM allows multiple clients to contribute to model training without direct personal data transfer to a central server. We assessed the performance of this model using real-world data from various clients navigating diverse paths. Metrics such as Root Mean Square Error (RMSE), Mean Absolute Error (MAE), and R-Square were employed for evaluation. A comparative study showed the FedLSTM's performance closely mirrored its centralized counterpart, with minor increases in RMSE and MAE. Further, we investigated the model's robustness with varying client participation and local training epochs. Notably, even devices with constrained computational capabilities could significantly partake in federated model training with limited epochs, while still achieving commendable results. Visualization of the Radio Environmental Maps (REM) underscored the resemblance between FedLSTM and centralized LSTM outputs. However, a distinguishing advantage of our proposed FedLSTM is its inherent capability to safeguard client data privacy, concurrently diminishing communication overhead and alleviating server load.
- **Chapter 4:** summarizes the thesis contributions and future research directions.

Chapter 2

Efficient Indoor Industrial Communication Architecture using hybrid Wi-Fi and PLC network

2.1 Introduction

Advancements in smart industrial environments are unequivocally intertwined with the rapid evolution of network infrastructures, poised to redefine operational paradigms and bolster efficiency [15–17]. Central to this transformation is the amalgamation of formidable communication networks such as Local Area Networks (LAN), Radio Frequency (RF) communications, ZigBee, and Wide Area Networks (WAN), each playing a crucial role in fostering a seamlessly integrated, responsive, and adaptive industrial ecosystem [18–20]. These network technologies, despite their individual merits, present intrinsic challenges such as signal dispersion and coverage limitations in expansive and structurally intricate industrial settings [5, 21–23]. The quest for optimized network performance, consequently, necessitates

the exploration of hybrid network architectures. Such architectures aim to harness the collective capabilities of existing wireless and wired technologies, thereby mitigating individual technological limitations and enhancing overall network robustness and reliability [21, 22]. In essence, the envisioning and realization of hybrid networks stand as a pivotal stride towards achieving sophisticated, cost-efficient, and high-performance communication infrastructures, imperative for the nuanced demands of contemporary smart industrial settings.

Power line communication has been extensively employed in recent years to develop broadband networks with high data transmission rates based on power grids [24, 25]. Power line communication (PLC) technology is increasingly used to provide high-speed broadband connectivity with minimal infrastructure costs. One major benefit of using PLC networks is the ability to reuse existing electrical wiring for communication, making it an attractive option for smart grid applications. As a result, research in this field is extensive. Additionally, smart city [26, 27], in-home automation [8, 28], and telemetry [24] applications can also take advantage of this technology, as it eliminates the need for new cabling and avoids wireless propagation issues. Furthermore, Power Line Communication (PLC) technology has demonstrated its efficiency and effectiveness in a wide range of applications, including both broadband (BB) and narrowband (NB) communication. With the growing popularity of IoT smart homes and the demand for seamless connectivity, the plug-and-play extenders based on PLC technology are becoming increasingly popular in the market. These devices offer a simple and easy installation process, providing users with a convenient and reliable solution for extending their home networks. [11].

Power Line Communication (PLC) technology is a promising solution for modern telecommunication providers to overcome various challenges, including achieving advantages in a shorter time [29]. One of the earliest attempts to utilize home's electrical wiring to transfer information between household devices was the CE bus (Consumer Electronic Bus)

power-line carrier technology [30]. The development of a high-speed power-line carrier (PLC) standard began with the establishment of the Data Networking Subcommittee R7.3 by the Consumer Electronics Association towards the end of 1999 [31]. The primary goal of PLC technology is to achieve data speeds of up to 20 Mbit/s over power-line connections. To ensure that this technology coexists with existing devices that use home power lines for communication, the HomePlug Alliance was established, which aimed to develop a low-cost technology [29]. This technology leverages the existing powerline to provide Ethernet-class data speeds at any power outlet. The data rates have increased significantly with the advancement of signal processing and modulation techniques [32]. As a result, several businesses and commercial infrastructures worldwide have established broadband Internet access and building networks using PLC technology. In addition to that, Powerline communication (PLC) networking offers advantages beyond home and building networks, including communication in transport systems that already have electrical deployment [33]. Therefore, PLC networks have been studied for in-vehicle communication as well. However, the use of PLC networks is not limited to these applications.

PLC networks have been proposed for various applications, including robotics [34], authentication, security systems in mining [35], health monitoring [36, 37], and inductive coupling [38, 39]. The broad range of potential applications and associated issues has attracted significant attention from the scientific community and industry, leading to numerous solutions and various regulation and standardization activities. In this paper, we investigate the feasibility of a hybrid broadband power line and Wi-Fi communication system in indoor industrial settings. The proposed system utilizes existing power line cables and Wi-Fi Plug-and-Play devices for indoor broadband connectivity. BPL (Broadband Power Line) adaptors with Wi-Fi outputs are used to construct an access network in industries, particularly in areas with weak wireless router signals. We demonstrate through a laboratory

experiment using the PLC Wi-Fi kit that a Wi-Fi and PLC hybrid network is well-suited for practical applications in an industrial context.

2.2 Network Structure

As in the Industrial environment certain data must be transferred and accessed across different units. The hybrid network architecture must have the ability to provide flexible network connectivity. To ensure optimal performance, the diagnostic data from network devices should be taken into consideration along with the service requirements of each medical application. In this industrial network, we utilized the two most widely used technologies - Wi-Fi and PLC - to build the access network. Our focus was on the access network characteristics created using the AV1000 Gigabit Power line Adapter kit. Specifically, in the industrial scenario illustrated in Figure 2.2, the Wi-Fi serves as the access point and is connected via Ethernet cable to the Tenda PH10 AV1000 AC WI-FI POWER LINE ADAPTER P3 (PLC Master Router) that is connected to the main distribution panel of the industrial electrical network. This master router spreads the signal via power lines to the PLC/Wi-Fi outlets connected to the same electrical network where the connected PLC Slaves catch the data signal and deliver it to the internet devices for remote monitoring and industrial management etc. The high-end powerline adapter kit, (Tenda PH10 AV1000 AC WI-FI POWER LINE ADAPTER) is a plug and play device that increases network coverage to the different departments and other locations where the router's wireless signal cannot reach. The powerline adapter kit includes two devices: AV1000 Gigabit Powerline Adapter and AV1000 ac Wi-Fi Powerline Extender, as shown in Figure 2.1a and 2.1b respectively. Tenda powerline adapter uses HomeplugAV2 Technology standards, which supports MIMO (Multiple Input Multiple Output) signaling with beamforming. This feature improves network

coverage throughout the industry, particularly on high attenuated channels [8]. Additionally, MIMO allows transmission on any two-wire pair within the three-wire configuration of Line, Neutral, and Protective earth. The kit also offers extended frequency bands and efficient notching, providing a maximum throughput of 1000Mbps on powerline and up to 200Mbps on wireless at the physical layer. Tenda PH10 AV1000 AC WI-FI POWER LINE kit supports all modern networking standards up to 802.11ac. The adaptor kit utilizes AC650 dual-band Wi-Fi technology, ensuring speeds of 433Mbps on the 5GHz band and 200Mbps on the 2.4GHz band [11].



(a) Tenda PLC P3 Adapter



(b) Tenda PLC PA7 Extender

Figure 2.1: Tenda PH10 AV1000 AC Wi-Fi Powerline Kit

The AV1000 ac Wi-Fi Powerline adapter features an Ethernet port for connecting it to the wireless or Wi-Fi router, while the AV1000 ac Wi-Fi Powerline Extender has an additional Gigabit Ethernet port for stable connections with wired devices such as remote monitoring equipments, cameras, printer, TV, HD set-top box, and so on [29]. The Tenda PH10 AV1000 ac Wi-Fi Powerline Extender Kit comprises the PA7 extender and a Tenda

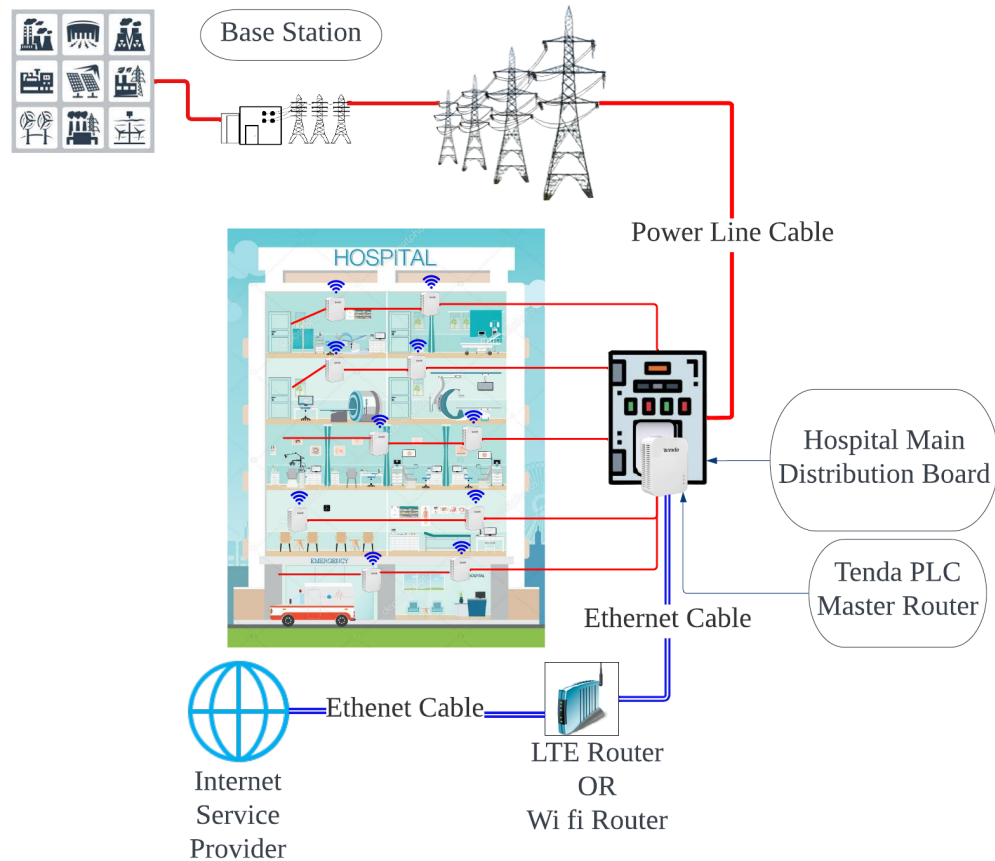


Figure 2.2: Industrial network design

P3 powerline adaptor. It is configured to use the Broadcom BCM47189B0 Chip in 2x 1x1:1 mode. The Broadcom BCM47189B0 Chip can be seen in Figure 2.3. Also, the device uses Broadcom BCM60350 as the HomePlug controller. The RAM Configuration is 1Gb (64M x 16) on Winbond chipset W631GG6KB -15. The AV1000 AC Wi-Fi Powerline Extender Kit is a set of PLC adapters that offer support for all modern networking standards from 802.11a to 802.11ac for 2.4GHz and 5GHz bandwidth with theoretical speed of 1000Mbps on PHY layer with 5GHz band (433Mbps) and 2.4GHz band (200Mbps). The maximum Power consumption of PA7 extender is 8.4W whereas the standby power is 4.7 W.

Similarly, the maximum power consumption of P3 adaptor is 3.2W and the minimum

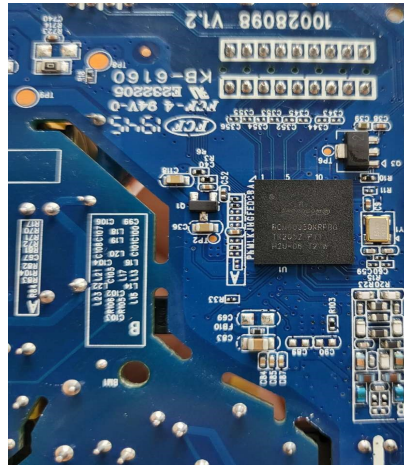


Figure 2.3: Broadcom BCM47189B0 chip

is 0.36W. The input power ranges from 100V to 240V for 50/60Hz power frequency. The Tenda PH10 AV1000 AC WI-FI POWER LINE adaptor kit makes the internet available to any area of a industrial building by sharing it wired or wireless with all internet devices within the industry. The unified network can maintain stable connectivity within industrial environment.

System Model

A system model was created to test the performance of the hybrid system in a laboratory. A PLC Master was connected to the ipTIME AX8008M Wi-Fi Router via Ethernet cable, which was then connected to a power line cable. We used electrical extension boards to adjust the length in accordance with our requirements and to place the PLC slaves at the specified location more accurately inside the network. The configuration of the network is shown in Figure 2.4a, 2.4b, and 2.4c for lengths of 10, 30, and 60 meters, respectively. The performance of the system was then analyzed using Startrinity CST setting the download and upload limitations to 1000 Mbps and 100 Mbps, respectively. The performance of the system was then analyzed using Startrinity CST setting the download

and upload limitations to 1000 Mbps and 100 Mbps, respectively.

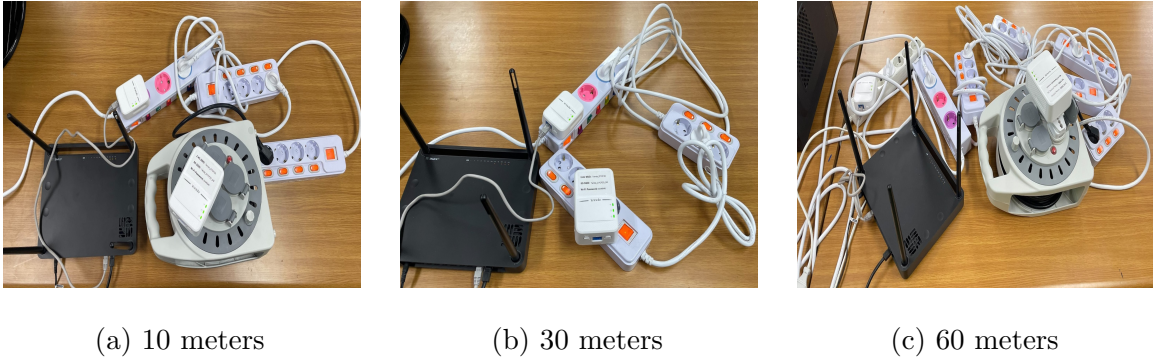


Figure 2.4: Laboratory system setup for different lengths

Startrinity CST is a tool that continuously measures internet speed and can do it for a very long period of time. Startrinity CST makes upload and download simultaneously and continuously unlike other tools that make upload for a set period of time and downloads for another set period. For such various tests, there may be different speed test results. For example, downloading a file can start at a higher speed, but the speed can drop after some time. Such degradation of internet quality is usually not detected by regular non-continuous speed tests tools. Round Trip Time (RTT), packet loss, and jitters can also be measured by the Startrinity CST. In this experiment, we restricted the upload and download speeds to 100 Mbps and 1000 Mbps, respectively. Figure 2.5 shows the measurement speed for 20 seconds while Figure 2.6 illustrates the home page of the Startinity CST.

2.3 Performance Analysis of The Hybrid Network of Wi-Fi and PLC

In order to test the performance at various locations, a hybrid PLC and Wi-Fi network was created in the university laboratory. The network structure is depicted in block

Home Measurements (compressed) (5) Measurements (raw) (150) Uptime 100.00%(0) Advanced													
Time	State	Download (Rx)	Upload (Tx)	Rx packet loss	Tx packet loss	RTT (ping)	Rx loss burst length	Tx loss burst length	Rx instant jitter	Tx instant jitter	Rx RFC3550 jitter	Tx RFC3550 jitter	
2022-09-26 22:11:36	up	107.29Mbps/1500.00Mbps	100.00Mbps/100.00Mbps	0.00%	0.00%	2.0ms	1.00 packet(s)	2.00 packet(s)	22.2ms	6.4ms	3.6ms	1.2ms	
2022-09-26 22:11:35	up	108.16Mbps/1500.00Mbps	100.00Mbps/100.00Mbps	0.00%	0.00%	2.0ms	1.00 packet(s)	2.00 packet(s)	26.5ms	2.4ms	4.0ms	0.7ms	
2022-09-26 22:11:34	up	107.79Mbps/1500.00Mbps	100.00Mbps/100.00Mbps	0.00%	0.00%	7.0ms	1.00 packet(s)	2.00 packet(s)	22.3ms	4.3ms	3.7ms	1.1ms	
2022-09-26 22:11:33	up	108.01Mbps/1500.00Mbps	100.00Mbps/100.00Mbps	0.00%	0.00%	2.0ms	1.00 packet(s)	2.00 packet(s)	25.2ms	3.1ms	4.0ms	0.8ms	
2022-09-26 22:11:32	up	107.74Mbps/1500.00Mbps	100.00Mbps/100.00Mbps	0.00%	0.00%	2.0ms	1.00 packet(s)	2.00 packet(s)	30.3ms	3.3ms	4.2ms	0.8ms	
2022-09-26 22:11:31	up	107.80Mbps/1500.00Mbps	100.00Mbps/100.00Mbps	0.00%	0.00%	7.0ms	1.00 packet(s)	2.00 packet(s)	12.9ms	1.9ms	3.8ms	0.6ms	
2022-09-26 22:11:30	up	107.18Mbps/1500.00Mbps	100.00Mbps/100.00Mbps	0.00%	0.00%	7.0ms	0.00 packet(s)	2.00 packet(s)	20.9ms	3.8ms	3.8ms	0.9ms	
2022-09-26 22:11:29	up	108.15Mbps/1500.00Mbps	100.00Mbps/100.00Mbps	0.00%	0.00%	7.0ms	0.00 packet(s)	2.00 packet(s)	22.8ms	3.1ms	3.5ms	0.9ms	
2022-09-26 22:11:28	up	108.01Mbps/1500.00Mbps	100.00Mbps/100.00Mbps	0.00%	0.00%	7.0ms	0.00 packet(s)	2.00 packet(s)	23.6ms	6.3ms	3.7ms	1.5ms	
2022-09-26 22:11:27	up	107.77Mbps/1500.00Mbps	100.00Mbps/100.00Mbps	0.00%	0.00%	6.0ms	0.00 packet(s)	2.00 packet(s)	14.4ms	3.0ms	2.8ms	1.0ms	
2022-09-26 22:11:26	up	107.10Mbps/1500.00Mbps	100.00Mbps/100.00Mbps	0.00%	0.00%	6.0ms	0.00 packet(s)	2.00 packet(s)	19.8ms	3.1ms	4.0ms	1.0ms	
2022-09-26 22:11:25	up	107.99Mbps/1500.00Mbps	100.00Mbps/100.00Mbps	0.00%	0.00%	6.0ms	0.00 packet(s)	2.00 packet(s)	22.3ms	5.2ms	4.1ms	1.0ms	
2022-09-26 22:11:24	up	107.96Mbps/1500.00Mbps	100.00Mbps/100.00Mbps	0.00%	0.00%	2.0ms	0.00 packet(s)	2.00 packet(s)	14.8ms	2.5ms	3.5ms	0.8ms	
2022-09-26 22:11:23	up	107.72Mbps/1500.00Mbps	100.00Mbps/100.00Mbps	0.00%	0.00%	2.0ms	0.00 packet(s)	2.00 packet(s)	13.5ms	2.9ms	2.6ms	0.8ms	
2022-09-26 22:11:22	up	108.62Mbps/1500.00Mbps	100.00Mbps/100.00Mbps	0.00%	0.00%	2.0ms	0.00 packet(s)	2.00 packet(s)	21.9ms	2.6ms	4.2ms	0.7ms	
2022-09-26 22:11:21	up	108.38Mbps/1500.00Mbps	100.00Mbps/100.00Mbps	0.00%	0.00%	6.0ms	0.00 packet(s)	2.00 packet(s)	18.2ms	2.4ms	3.4ms	0.7ms	
2022-09-26 22:11:20	up	107.90Mbps/1500.00Mbps	100.00Mbps/100.00Mbps	0.00%	0.00%	2.0ms	0.00 packet(s)	2.00 packet(s)	23.0ms	6.7ms	3.7ms	1.3ms	
2022-09-26 22:11:19	up	107.51Mbps/1500.00Mbps	100.00Mbps/100.00Mbps	0.00%	0.00%	2.0ms	0.00 packet(s)	2.00 packet(s)	20.7ms	2.7ms	3.4ms	1.1ms	
2022-09-26 22:11:18	up	107.32Mbps/1500.00Mbps	100.00Mbps/100.00Mbps	0.00%	0.00%	2.0ms	0.00 packet(s)	2.00 packet(s)	21.4ms	6.1ms	3.2ms	1.1ms	
2022-09-26 22:11:17	up	108.30Mbps/1500.00Mbps	99.99Mbps/100.00Mbps	0.00%	0.00%	2.0ms	0.00 packet(s)	2.00 packet(s)	25.4ms	6.6ms	4.5ms	1.1ms	
2022-09-26 22:11:16	up	108.00Mbps/1500.00Mbps	99.99Mbps/100.00Mbps	0.00%	0.00%	2.0ms	0.00 packet(s)	2.00 packet(s)	25.7ms	2.1ms	3.7ms	0.7ms	
2022-09-26 22:11:15	up	107.79Mbps/1500.00Mbps	99.99Mbps/100.00Mbps	0.00%	0.00%	3.0ms	0.00 packet(s)	2.00 packet(s)	19.2ms	2.7ms	3.3ms	0.9ms	
2022-09-26 22:11:14	up	107.56Mbps/1500.00Mbps	99.98Mbps/100.00Mbps	0.00%	0.00%	7.0ms	0.00 packet(s)	2.00 packet(s)	22.2ms	1.8ms	3.3ms	0.5ms	
2022-09-26 22:11:13	up	107.67Mbps/1500.00Mbps	99.98Mbps/100.00Mbps	0.00%	0.00%	3.0ms	0.00 packet(s)	2.00 packet(s)	31.5ms	26.8ms	4.9ms	3.5ms	
2022-09-26 22:11:12	up	108.41Mbps/1500.00Mbps	99.99Mbps/100.00Mbps	0.00%	0.00%	3.0ms	0.00 packet(s)	2.00 packet(s)	22.7ms	2.8ms	3.7ms	0.8ms	
2022-09-26 22:11:11	up	108.33Mbps/1500.00Mbps	99.99Mbps/100.00Mbps	0.00%	0.00%	6.0ms	0.00 packet(s)	2.00 packet(s)	31.1ms	3.6ms	4.5ms	0.9ms	
2022-09-26 22:11:10	up	108.18Mbps/1500.00Mbps	100.00Mbps/100.00Mbps	0.00%	0.00%	3.0ms	0.00 packet(s)	2.00 packet(s)	20.5ms	5.1ms	3.7ms	1.2ms	
2022-09-26 22:11:09	up	107.89Mbps/1500.00Mbps	100.00Mbps/100.00Mbps	0.00%	0.00%	2.0ms	0.00 packet(s)	2.00 packet(s)	18.6ms	6.3ms	3.6ms	1.3ms	
2022-09-26 22:11:08	up	107.42Mbps/1500.00Mbps	99.98Mbps/100.00Mbps	0.00%	0.00%	2.0ms	0.00 packet(s)	2.00 packet(s)	19.8ms	2.9ms	3.0ms	0.8ms	
2022-09-26 22:11:07	up	107.43Mbps/1500.00Mbps	100.00Mbps/100.00Mbps	0.00%	0.00%	2.0ms	0.00 packet(s)	2.00 packet(s)	15.5ms	5.2ms	2.9ms	1.1ms	
2022-09-26 22:11:06	up	107.21Mbps/1500.00Mbps	100.00Mbps/100.00Mbps	0.00%	0.00%	2.0ms	0.00 packet(s)	2.00 packet(s)	18.5ms	2.7ms	3.3ms	1.0ms	
2022-09-26 22:11:05	up	106.68Mbps/1500.00Mbps	100.00Mbps/100.00Mbps	0.00%	0.00%	2.0ms	0.00 packet(s)	2.00 packet(s)	30.2ms	2.4ms	4.1ms	1.1ms	
2022-09-26 22:11:04	up	106.40Mbps/1500.00Mbps	100.00Mbps/100.00Mbps	0.00%	0.00%	8.0ms	0.00 packet(s)	2.00 packet(s)	20.9ms	5.3ms	3.7ms	1.0ms	
2022-09-26 22:11:03	up	107.46Mbps/1500.00Mbps	100.00Mbps/100.00Mbps	0.00%	0.00%	7.0ms	0.00 packet(s)	2.00 packet(s)	21.2ms	3.5ms	3.3ms	1.0ms	
2022-09-26 22:11:01	up	108.42Mbps/1500.00Mbps	100.00Mbps/100.00Mbps	0.00%	0.00%	3.0ms	0.00 packet(s)	2.00 packet(s)	25.0ms	5.1ms	3.6ms	1.2ms	
2022-09-26 22:11:00	up	108.28Mbps/1500.00Mbps	100.00Mbps/100.00Mbps	0.00%	0.00%	3.0ms	0.00 packet(s)	2.00 packet(s)	15.9ms	2.6ms	2.5ms	0.8ms	
2022-09-26 22:10:59	up	108.24Mbps/1500.00Mbps	100.00Mbps/100.00Mbps	0.00%	0.00%	2.0ms	0.00 packet(s)	2.00 packet(s)	15.9ms	3.3ms	3.2ms	0.8ms	
2022-09-26 22:10:58	up	107.84Mbps/1500.00Mbps	100.00Mbps/100.00Mbps	0.00%	0.00%	2.0ms	0.00 packet(s)	2.00 packet(s)	21.2ms	2.0ms	3.5ms	1.2ms	
2022-09-26 22:10:57	up	107.23Mbps/1500.00Mbps	100.00Mbps/100.00Mbps	0.00%	0.00%	3.0ms	0.00 packet(s)	2.00 packet(s)	23.8ms	8.7ms	3.8ms	1.5ms	
2022-09-26 22:10:56	up	108.31Mbps/1500.00Mbps	100.00Mbps/100.00Mbps	0.00%	0.00%	7.0ms	0.00 packet(s)	2.00 packet(s)	25.1ms	3.0ms	3.8ms	0.8ms	
2022-09-26 22:10:55	up	107.92Mbps/1500.00Mbps	100.00Mbps/100.00Mbps	0.00%	0.00%	8.0ms	0.00 packet(s)	2.00 packet(s)	23.2ms	4.2ms	3.2ms	1.0ms	
2022-09-26 22:10:54	up	107.91Mbps/1500.00Mbps	100.00Mbps/100.00Mbps	0.00%	0.00%	7.0ms	0.00 packet(s)	2.00 packet(s)	20.1ms	8.3ms	3.3ms	1.2ms	
2022-09-26 22:10:53	up	107.44Mbps/1500.00Mbps	100.00Mbps/100.00Mbps	0.00%	0.00%	7.0ms	0.00 packet(s)	2.00 packet(s)	18.5ms	2.2ms	3.0ms	0.8ms	
2022-09-26 22:10:52	up	107.64Mbps/1500.00Mbps	100.00Mbps/100.00Mbps	0.00%	0.00%	3.0ms	0.00 packet(s)	2.00 packet(s)	14.9ms	2.9ms	2.9ms	0.9ms	
2022-09-26 22:10:51	up	108.58Mbps/1500.00Mbps	100.00Mbps/100.00Mbps	0.00%	0.00%	3.0ms	0.00 packet(s)	2.00 packet(s)	15.7ms	3.0ms	2.8ms	1.3ms	

Figure 2.5: Measurement Results

diagram shown in Figure 2.7. We connected a Tenda PLC Master (P3) by Ethernet Cable to the ipTIME AX8008M Wi-Fi router, which serves as a network access point, and then to the Internet Service Provider (ISP). After that, we linked the Tenda PLC Slave (PA7) to the Tenda PLC Master (PA3) via electrical power line extensions at three different distances i.e., 10, 30, and 60 meters, and we individually analyzed the results. Figure 2.8 shows the measurement points and physical distribution of the extenders. The Tenda P3 transmits the signal via power lines throughout the electrical network and the Tenda PA7 extenders catch the transmitted signal and spread it to the end devices where it can be used for different

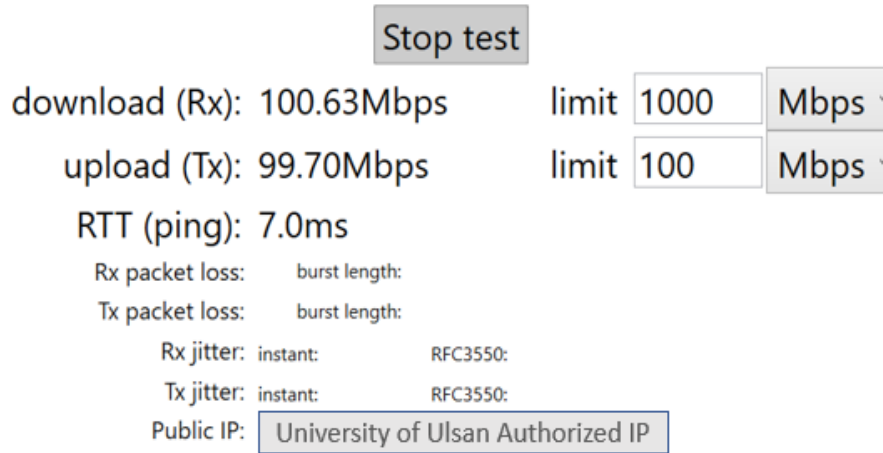


Figure 2.6: Startrinity CST home Page

industrial applications. We performed the experiments by considering the 3 points namely, point 3, point 2 and point 5 that are located at distance 10, 30 and 60 meters respectively. The access point is situated at point A. A Lenovo G50- 80 laptop and StarTrinity software is used to measure the different parameters of the network. StarTrinity CST measures the different parameters of the network continuously from where a .CSV file can be generated to extract different features of the network. For plotting we used matplotlib.pyplot Python library.

2.3.1 Throughput Measurement

We set up the Tenda PA7 Wi-Fi Extender in 5G mode and operated it at points 3, 2, and 5 individually in order to assess the throughput at various locations. To create a .CSV file for further analysis, we continually measured the bit rate for 150 seconds using StarTrinity CST (Continuous Internet Speed Test). Overall, Figure 2.9 shows that the bit rate drops gradually when the PA7 extender is moved away from the main router. First, the PA7 extender was connected to the master router via Power-Line cable at a distance of 10 meters. The graph depicts that the average throughput was calculated to be 88.20 Mbps,

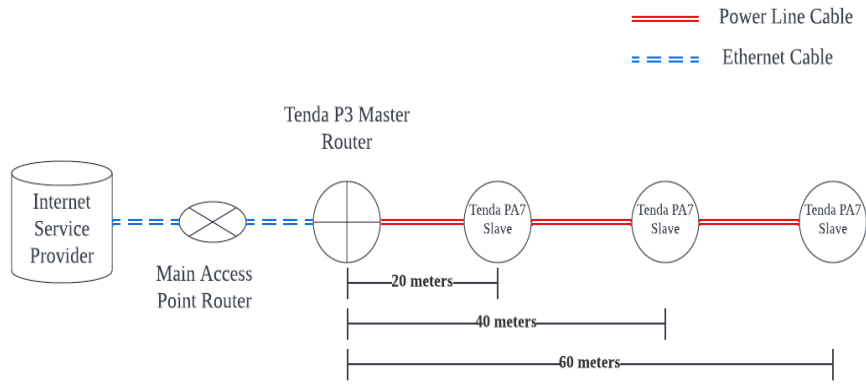


Figure 2.7: System configuration

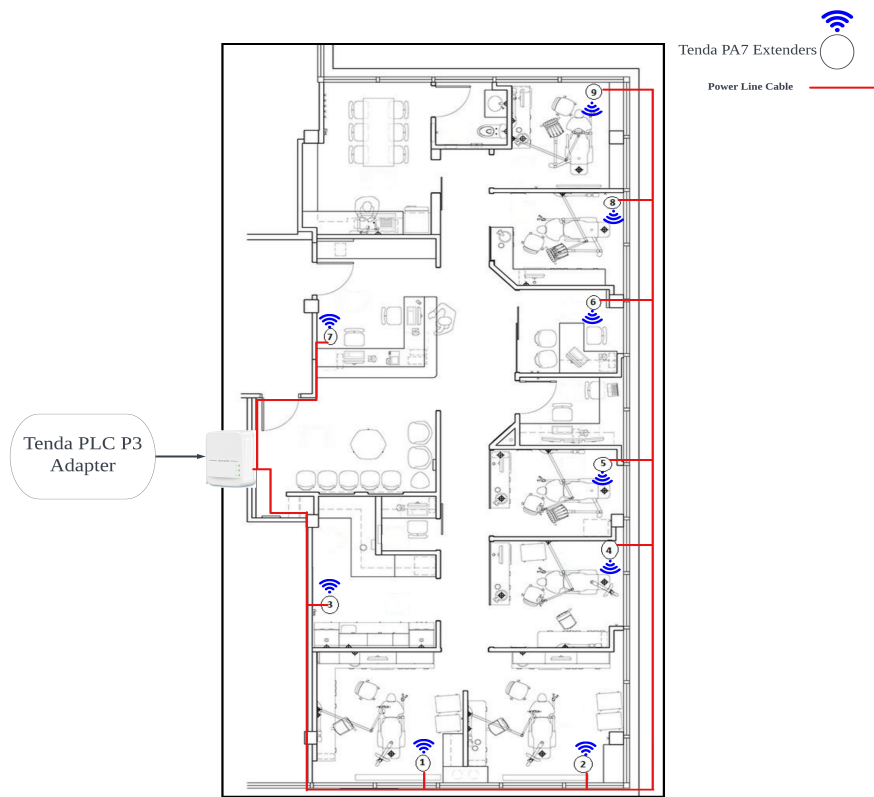


Figure 2.8: Location point within industrial network

while the lowest and highest speeds were recorded at 77.14 and 94.91 Mbps, respectively. After that, we extended the Power-Line Cable to point 2, which was 30 meters distant from the main router, and connected the PA7 to the P3 adapter there. We then monitored the data rate for an additional 150 seconds. It was seen that the lowest and maximum speeds decreased to 75.25 Mbps, respectively, and that of the average speed reduced to 80 Mbps. Finally, when the PA7 extender was extended to point 5, The average bit rate decreased further to 77.12 Mbps, with the lowest being 62.35 Mbps and the maximum being 77.01 Mbps.

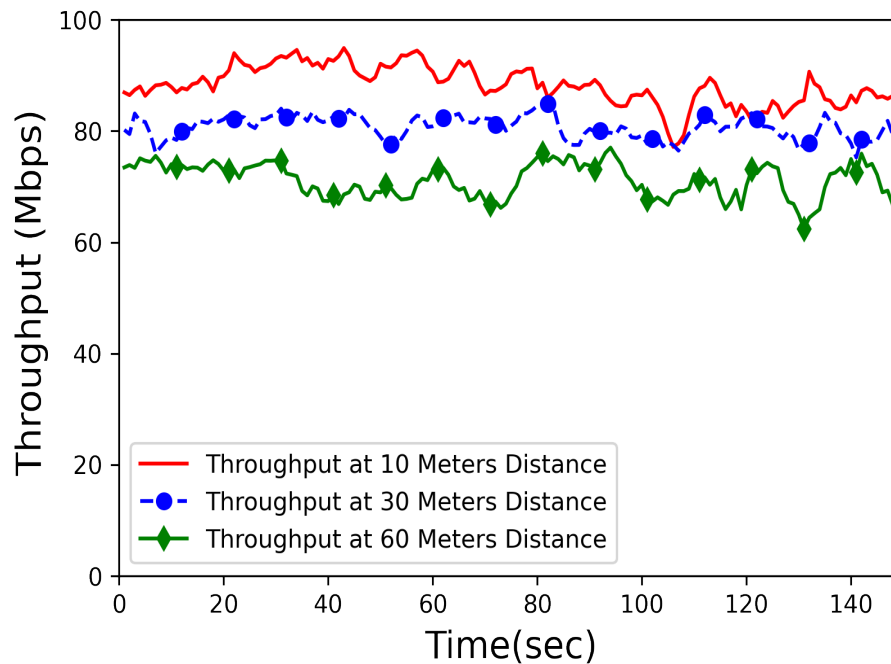
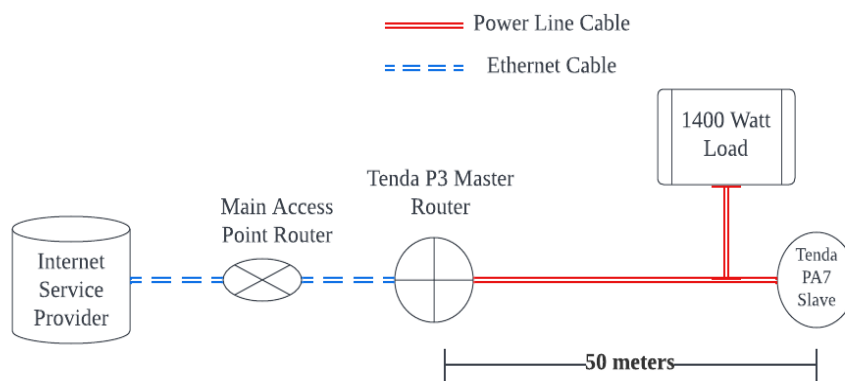


Figure 2.9: Throughput variation with length

2.3.2 Effect of Load on Tenda PA7 Powerline Extender

We initially evaluated the Ph10 Power line adapter kit's performance in lines with no load, after which we attached some load to the electrical network and retested the

performance. The main access router was connected to the Tenda. We initially evaluated the Ph10 Power line adapter kit's performance in lines with no load, after which we attached some load to the electrical network and retested the performance. The main access router was connected to the Tenda PLC Master (PA3), which was then linked to the Tenda PLC slave (PA7).



(a) Block diagram



(b) Laboratorial setup

Figure 2.10: 1400-Watt load connection

As illustrated in Figure 2.10a, the configuration was created for a single point where the Tenda PA7 and Tenda PA3 were placed 50 meters apart and a 1400-watt load was injected into the network. The real laboratory set-up is depicted in Figure 2.10b, and

performance in both scenarios was examined. In order to Figure out how the load impacted the extender's performance; the throughput was monitored for 150 seconds. The graph in Figure 2.11 shows that the first case's average data rate was 70.7Mbps, with a lowest of 61.45 Mbps and a highest of 76.35 Mbps. However, the minimum and maximum data rates declined to 48.98 Mbps and 73.52 Mbps, respectively, while the average rate decreased to 65.97Mbps.

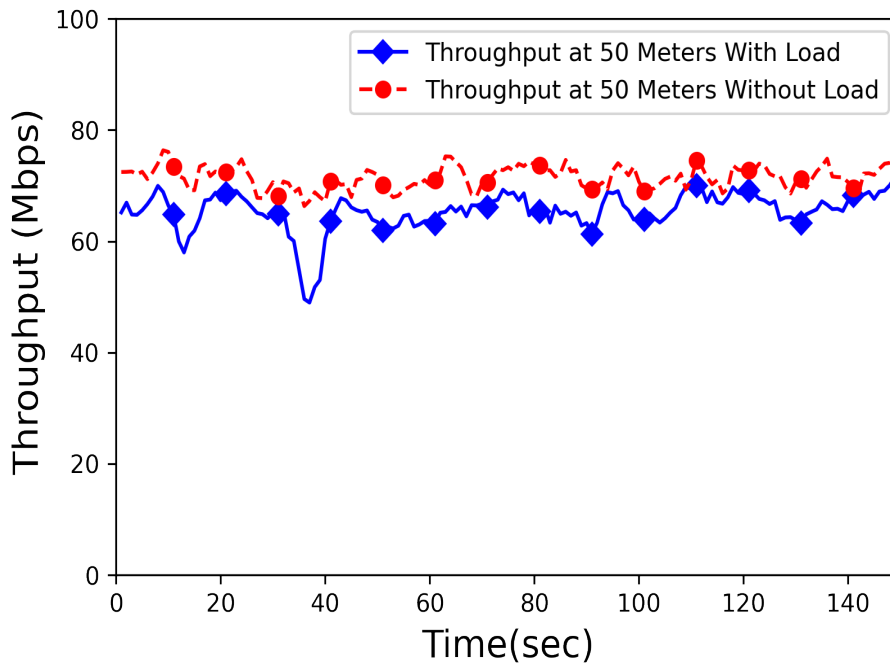


Figure 2.11: Performance of Tenda P10 with and without load

2.3.3 Signal Strength Analysis

To analyze the Received Signal Strength a Wi-Fi Analyzer Android application was used. Figure 2.12a illustrates that at 20-meter distance the main router's signal strength was below -60dbm, however, this strength was above -30dbm for the Tenda PA7 PLC extender. Then, we extended the powerline extension to 25 meters and analyzed the signal strength of

the Tenda P10 Tool Kit and the main router's signal at that point. The Signal strength of the main router's signal was observed to be below -90 dBm compared to the Tenda PA10 Tool Kit's signal strength which was just below -40 dBm as shown in Figure 2.12b. After that, we further extended the extension to 30 meters distance. Figure 2.12c shows that at 30 meters distance the main access point router has no signal power to be shown on mobile application but the Tenda P10 toolkit had a signal strength of above -30 dBm.

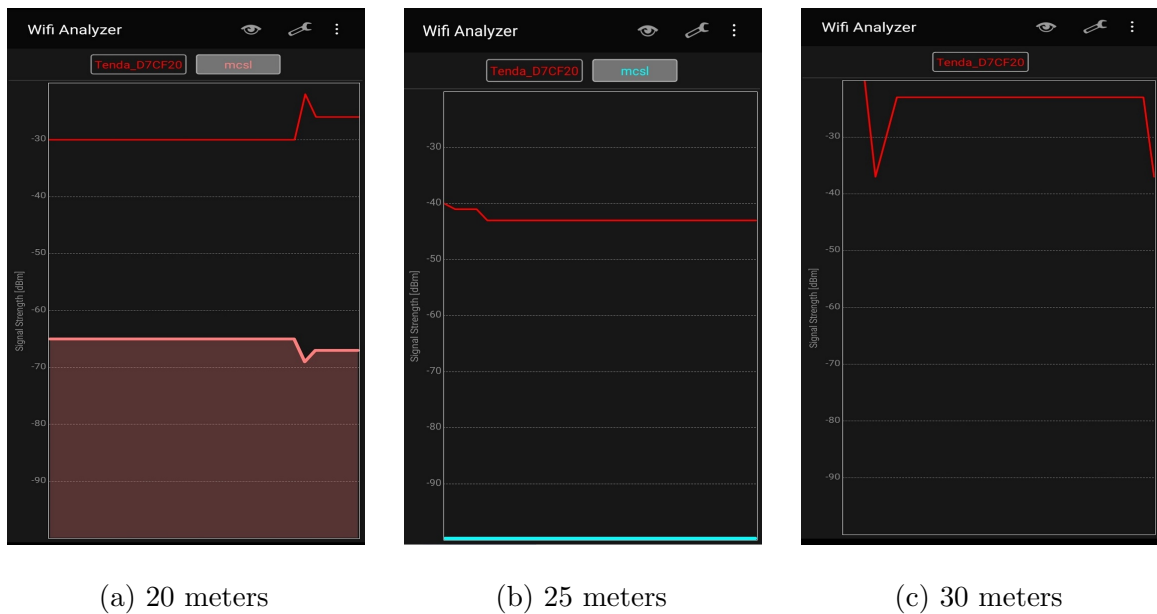


Figure 2.12: Signal strength analysis at different distances

2.4 Applications and features of the hybrid system

2.4.1 Features

The hybrid system integrates the robust capabilities of both the PLC and Wi-Fi technologies, formulating a multifaceted solution adeptly suited for diverse industrial scenarios. Specifically, the hybrid system encompasses the subsequent functionalities:

Locatable

In a versatile industrial environment, the hybrid system optimally leverages the ubiquitous presence of electrical wiring for enhanced indoor positioning capabilities. The integrated PLC network can seamlessly synchronize with existing tracking or monitoring systems, providing a unified solution for power and communication needs. This integration between PLC and Wi-Fi technologies can be instrumental in delivering a spectrum of indoor location-based services essential for modern industrial operations, including precise indoor navigation, emergency response coordination, and various other functionalities that bolster operational efficiency and safety.

Mobility

The Tenda PLC P10 Power Line Kit exemplifies operational agility owing to its plug-and-play nature and the pervasive deployment of electrical wiring throughout industrial environments. Such a design enables facile repositioning of the PA7 extenders within a unified electrical network, allowing for strategic placement and relocation based on evolving operational demands, thereby ensuring uninterrupted and optimized connectivity across various locational nodes within the industrial setting.

Radiation-Free

In industrial environments, mitigating unnecessary electromagnetic interference is crucial to maintain the integrity and performance of various equipment and machinery. Utilizing 3G/4G networks can introduce such interferences, potentially disrupting operational efficiency. The PLC system emerges as a superior alternative, enabling the transfer of high data rates without the associated radiation leakage, thus safeguarding the operational environment from potential electromagnetic disruptions and maintaining a consistent

performance standard across various industrial applications.

High Capacity

The hybrid configuration is proficiently engineered to attain data transmission rates soaring up to 1000 Mbps, marking a substantial amplification in the system's overall data handling capacity. In a dynamic industrial setting populated with multiple concurrent users and characterized by necessities for substantial, sporadic data transmissions, the augmented capacity is instrumental. It seamlessly facilitates operations, such as the efficient handling of voluminous data sets, supporting high-resolution video conferencing, and ensuring the swift and reliable transfer of essential operational data, aligning with the diverse and demanding requirements of a modern industrial ecosystem.

Data Security

Utilizing power line cables as the communication backbone, the hybrid system enhances the security posture of data transmissions within the network. This approach confines data exchange within the same electrical network, bolstering the integrity and confidentiality of the information as it traverses various sectors within the industrial environment. Such a secured communication pathway is instrumental in protecting sensitive operational data from potential vulnerabilities and unauthorized access.

2.4.2 Possible Applications

Upon a meticulous evaluation of all intrinsic features of the proposed system, a tangible demonstration employing the foundational methods has been actualized within a lab setting, as depicted in Fig. 4. The manifold applications of this hybrid system can be broadly categorized into two distinct groups, each aligning with their respective utilitarian

functions and operational requisites.

Medical Uses

The system has the capability to offer various medical services through the integration of a robust network protocol. These services include patient data record maintenance, efficient data management and transfer services, remote patient vital sign monitoring, telemedicine or remote consultation services, immediate pathological image analysis through diagnostic video conference, remote surgeries, and several other services.

Non-Medical Uses

The hybrid proposed system is versatile and can also offer various non-medical services. These services include emergency broadcasting, managing indoor navigation equipment, transmitting multimedia content for entertainment, controlling smart community devices such as smart clocks, LED lights, and online attendance, etc.

2.5 Conclusion

In this chapter, we explore potential applications for a hybrid broadband power line and Wi-Fi communication system in indoor industrial scenarios. The system utilizes the already existing power line cables and Wi-Fi Plug-and-Play devices for indoor broadband communication. Moreover, we discussed the effect of load and Powerline cable length on the Tenda PH10 AV1000 AC Wi-Fi Powerline Extender Kit. First, we transferred the 100Mbps data from master router to the slaves placed at distances of 10, 30,60 meters and calculated the download Mbps. It was concluded that the data rate decreased slightly when the length of the power line cable increases. Also, the load also has a minimal effect on data rate when compared with the no load power line. However, the proposed hybrid system

has several excellent features, including, High capacity, strong privacy and security, and impending availability. We do believe that using a hybrid system in a industrial setting can emphasize its benefits, and we are hopeful that doing so would increase interest in e-health research groups while also supporting applications for indoor industries. The selected Power Line Communication (PLC) and Wi-Fi Kit incorporates all the current Wi-Fi technologies and implements the widely adopted HomePlug AV2 specification for broadband power line systems. The achieved results demonstrate the feasibility of using these devices for indoor applications in industries, making them a suitable choice for building access networks. In our future work we are planning to design smart beds for Intensive Care Units(ICU) using Power Line and Wi-Fi standards.

Chapter 3

Radio Environment Map

Construction based on

Privacy-centric Federated Learning

3.1 Introduction

Awareness of operating environment conditions is progressively becoming an important supplementary aspect for efficiently managing resources in diverse dynamic systems. This is particularly evident in the context of the Fourth Industrial Revolution. This era has ushered in advanced technologies like artificial intelligence, big data, the Internet of Things (IoT), and robotics, which have been deployed in smart factories. These factories automate production processes, thereby facilitating automatic assessment of process status and enabling timely interventions [12].

Central to the functionality of smart factories is wireless communications, which assumes a pivotal role in empowering instantaneous tracking and surveillance of production

processes. Moreover, the flexibility and simplicity of wireless communications make it the preferred mode of connectivity in the dynamic landscape of production environments, compared to cumbersome wired alternatives. However, the surging count of wireless devices introduces a challenge—potential interference with the industrial, scientific, and medical (ISM) band [13]. Moreover, obstacles within indoor environments can attenuate communication signals, leading to regions of radio shadow. Accordingly, a precise assessment of the extent of radio communication coverage emerges as a priority. In addressing the aforementioned challenge, radio environment map (REM) construction has been investigated as an innovative tool that serves to furnish intricate details about the radio environment within specific geographic areas. By harnessing the insights provided by the REM, informed decision-making is facilitated, and network operators can seamlessly identify coverage gaps and high-traffic regions [14].

In the literature, path loss models have been investigated for coverage prediction. However, these models depend on various factors, such as the distance between transmitter and receiver as well as the height of the receiver and transmitter above ground, which increases the difference in error prediction between real and estimated values [40]. Hence, machine learning (ML)-based approaches have emerged as innovative predictive methods capable of effectively addressing the intricate operational challenges within communication networks. These techniques have demonstrated a remarkable ability to achieve high prediction accuracy [41, 42]. For instance, researchers have projected the path loss in an urban setting in Beijing, China, when utilizing artificial neural networks (ANNs), support vector regression (SVR), and random forest (RF) models [43]. Assessments of performance were measured through root mean square error (RMSE), yielding results ranging between 4 dB and 5 dB. In [44], the authors proposed the extra tree regressor-based approach for REM construction in wireless communications networks for indoor environments. The results showed that

the extra tree regressor can obtain the best accuracy with less computational time than other ensemble learning baseline schemes. To the best of our knowledge, the researchers described above considered a centralized manner where the learning process is managed by a central server or a base station. In this paper, we propose a federated learning (FL) approach called FedLSTM, which works with a long short-term memory (LSTM) model to provide distributed learning between users. Note that in the conventional centralized approach, more data are transmitted since both the features and the labels must be sent. On the other hand, in a distributed manner, the user only sends the weights of the local model that are entailed in computation.

Moreover, the proposed FedLSTM scheme allows both server and users to generate the REM. Then, the server can be considered network planning to obtain a REM that can solve coverage problems (installing APs or relays). Meanwhile, users can more fully appreciate coverage of the area, and can redirect to a better coverage area by looking at the REM. In addition, the proposed FL-based approach provides security because the data sent to the server are the weights, not the labels and features of each user. This scenario is very useful in commercial, hospital, and military environments where users do not want to share their location with unknown people, thus guaranteeing privacy and security.

We propose a novel FL-based approach to coverage prediction in indoor environments that not only minimizes data transmission but also enables network planning and empowers users to make informed decisions about their coverage. Additionally, it prioritizes user privacy and security, making it highly applicable in various sensitive settings

The main contributions of this paper can be summarized as follows.

- First, we propose a novel FL-based approach, called FedLSTM, providing coverage prediction for indoor environments. FedLSTM enables distributed model training by having users send only model weights to the server. This is in stark contrast to

centralized approaches where users must transmit both features and labels, leading to a significant increase in data transmissions.

- Secondly, the data utilized in this study were collected from a real environment with location points captured using Emesent’s Hovermap and real received signal strength indicator (RSSI) values obtained via Raspberry Pi. After collection, we preprocess the location data with Emesent’s software and synchronize it with the cleaned RSSI readings from Raspberry Pi by using timestamps.
- Third, we construct a REM by using Python software to enhance coverage prediction visualization. For this objective, we generate a grid of data comprising 1000×1000 grid points within our area of interest to plot coverage prediction over a 2D map.
- Furthermore, our FL-based scheme empowers both server and users to generate the REM. The server functions as the network planner, leveraging the REM to address coverage issues by installing access points or relays. On the other hand, users can assess the coverage of their area and relocate to areas with better coverage by examining the REM.
- In addition, we compared the FedLSTM model with its centralized counterpart, showing that our research ensures security by transmitting only the weights of each user’s model to the server, while the labels and features remain private. This approach is particularly advantageous in commercial, hospital, and military settings where users are hesitant to share their location data with unknown entities.

3.2 Related Work

Radio maps (commonly known as REMs) and their construction play a very important role in modern communication systems. These maps offer a comprehensive view of

the radio spectrum environment by retaining various types of information, from geographic and land features to spectrum usage characteristics. Over the years, a significant amount of research has been conducted to enhance and diversify their applications. Introduced in 2006 [45], REMs have facilitated a multitude of applications, ranging from network monitoring [46], localization [47] and resource management [48] to V2X communication [49, 50].

Traditional methods of radio map construction often involve detailed field surveys, which can be time-consuming and labor-intensive. To address this, researchers have been developing algorithms to lower these costs. A number of path loss models have been influenced by factors like terrain suitability, the heights of the receiver and transmitter above ground level, their spatial [51]. These elements can widen the gap between forecast and real signal degradation, with the extent of the variance hinging on the chosen propagation model. In the REM construction literature, ordinary kriging (OK) is frequently employed as a geostatistics-based spatial interpolation method [52, 53]. OK predicts unseen data points by considering the spatial relationships between recorded data and the relative locations of all sampled points [54]

In [55] Maiti and Mitra developed a radio map for indoor signal propagation, leveraging interpolation methodologies. Results showed that OK achieved better performance than ordinary methods like inverse distance weighting [56] and K-nearest neighbors (KNN). These methods were evaluated based on prediction error, i.e., RMSE. Although the OK-based model achieved better performance, it encounters a limitation in its computational proficiency, especially with more data points [57].

In [57], and [58], heuristic-derived methodologies were introduced providing indoor coverage prediction for indoor dominant path models. However, heuristic solutions are typically designed for specific problems, and might not generalize well to other scenarios or variations of the problem, making them inconsistent and unreliable in critical applications.

In classical prediction models, the design of mobile-device networks demonstrates an inherent lack of adaptability [59]. Predictions are constrained to specific conditions, such as frequency range, antenna height, and surrounding environmental conditions. Nonetheless, current observations indicate that the operational environment of modern radio networks is characterized by an elevated level of diversity and complexity [60]. Consequently, there is a strong need for prediction models that are more flexible and that can handle the challenges of modern networks.

ML-based prediction techniques are recognized as revolutionary within the realm of modern mobile-device network planning owing to their enhanced accuracy over age-old empirical prediction methods. When compared with deterministic-based models, the ML-based methods are notably superior in their data processing efficacy [61, 62].

For instance, the authors in [63] conducted research in an urban area of Lisbon, Portugal, at 3.7 GHz and 26 GHz frequency bands, leveraging an authentic 5G network. They utilized input factors, and the resultant values closely matched those in [43]. However, the dataset utilized was double in size. The study mainly focused on SVR and RF models, which showed error rates ranging between 6 dB to 7 dB.

Similarly, the authors in [64] conducted their research in suburban areas of South Korea, focusing on frequency bands of 450 MHz, 1450 MHz, and 2300 MHz. Although the input parameters were mostly similar to previous studies, a new parameter was introduced: the ratio between Tx height and Rx height. That research exclusively employed the Artificial Neural Network (ANN) and Gaussian Process Regression (GPR) ML models, both of which exhibited RMSE values ranging from 8 dB to 9 dB.

Lastly, the authors in [65] introduced a new approach using the extremely randomized trees regressor (ERTR) algorithm for mobile coverage prediction, and visualized results on a REM overlaid on top of Google Earth. Real measurement data from Victoria Island

and Ikoyi in Lagos, Nigeria, were used. Through extensive simulations and comparisons with seven other ML algorithms, including ordinary kriging, the ERTR algorithm showed the lowest RMSE error at 2.75 dB with an R^2 score of 92

Lastly, the author in [66] introduced a new approach using the extremely randomized trees regressor (ERTR) algorithm for mobile coverage prediction and visualizes results on a REM overlaid on Google Earth. Real measurement data from Victoria Island and Ikoyi in Lagos, Nigeria was used. Through extensive simulations and comparisons with seven other ML algorithms, including ordinary kriging, the ERTR algorithm showed the lowest RMSE error of 2.75 dB with R-2 score of 92%.

To the best of our knowledge, commonly employed methods for constructing radio maps heavily rely on centralized data approaches. While these methods are comprehensive, they bring forth computational complexities and potential vulnerabilities, particularly concerning user-specific data such as geospatial information. In environments such as commercial complexes, healthcare institutions, and military facilities, the adoption of a centralized approach is considered suboptimal. In these contexts, users place a high premium on privacy and security, necessitating measures to prevent the disclosure of location information to unauthorized parties. Our model incorporates the FL approach, advocating decentralized data processing across user nodes. Unlike the centralized framework, which necessitates transmission of both feature vectors and labels, the federated approach entails only transmission of model weight vectors. This reduction in data transmission overhead simultaneously enhances data security for users, with a minimal increase in prediction error.

3.3 Data Collection and Preprocessing

In this study, we sourced our primary data from the Engineering Building at the University of Ulsan in South Korea. For the collection process, we systematically employed two key devices: the Emesent Hovermap and Raspberry Pi.

3.3.1 Emesent Hovermap

Emesent Hovermap, shown in Figure 3.1, is a cutting-edge LiDAR mapping and autonomy payload designed for drones. It facilitates the capture of high-resolution, 3D spatial data in environments where GPS signals may be unreliable or non-existent, such as underground mines, dense forests, or indoors. Powered by Emesent's proprietary SLAM (Simultaneous Localization and Mapping) algorithm, Hovermap allows drones to navigate autonomously, avoid obstacles, and ensure safe flight in challenging terrains.



Figure 3.1: EMESENT Hovermap

What sets Hovermap apart is its ability to transform the way industries like mining, infrastructure, and forestry collect and utilize data, promoting safer and more efficient operations. With its advanced features and capabilities, Hovermap is establishing itself as a

game-changer in the domain of drone-based LiDAR mapping. The Emesent Hovermap is equipped with three distinct ports, two specialized antennas, and a dedicated power button, each serving specific functions as outlined below. A detailed depiction of these components can be found in Figure 3.2.

- **USB Port:** This port facilitates fast data transfer and connectivity. It's commonly used to upload or download data, update firmware, or connect the device to external computing resources.
- **Serial Port:** A communication interface that allows the Hover Map to connect with other hardware devices or controllers. The serial port is crucial for real-time data transmission, especially in applications where timing is critical.
- **Power Port:** As the name suggests, this port is used to charge the device or provide continuous power during operation. Ensuring a reliable power source is essential for the uninterrupted functioning of the Hover Map.
- **Status LED:** A light-emitting diode (LED) that provides visual feedback about the device's operational status. By observing the LED's behavior (such as blinking patterns or color changes), users can quickly determine if the device is working correctly or if there are any issues.
- **Power Button:** A tactile button used to turn the Hover Map on or off. It might also have additional functionalities like resetting the device or initiating specific modes when pressed in certain sequences.
- **Antennas:** These are essential for ensuring strong wireless communication. The antennas on the Hover Map likely enhance its capability to send and receive data, especially in environments where signal strength might be compromised.

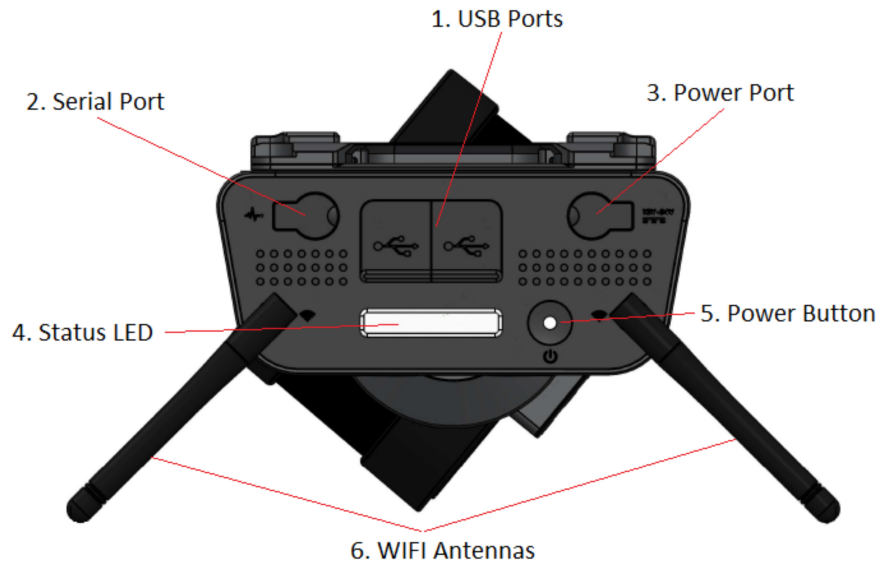


Figure 3.2: EMESENT Hovermap Rear View

3.3.2 SLAM Distance Measurement via LiDAR

LiDAR, which stands for Light Detection and Ranging, is a remote sensing method that uses light in the form of a pulsed laser to measure distances to objects on the ground, in the water, or in the atmosphere. The fundamental principle behind LiDAR involves emitting laser pulses and then measuring the time it takes for the emitted light to travel to the target and reflect back to the sensor. This time, often referred to as the 'time of flight', when combined with the known speed of light, gives a direct measure of the distance between the sensor and the object. In the context of SLAM (Simultaneous Localization and Mapping), which is a computational problem of constructing or updating a map of an unknown environment while simultaneously keeping track of an agent's location within it, LiDAR can be pivotal. The high-resolution distance data from LiDAR can be used by SLAM algorithms to identify and map structures in the environment while also determining the sensor's position within this environment. This simultaneous ability to map and localize

using accurate distance measurements makes LiDAR an invaluable tool in applications like autonomous driving, robotics, and topographical mapping. The cloud map of room 611, at university of Ulsan, is shown in figure 3.3

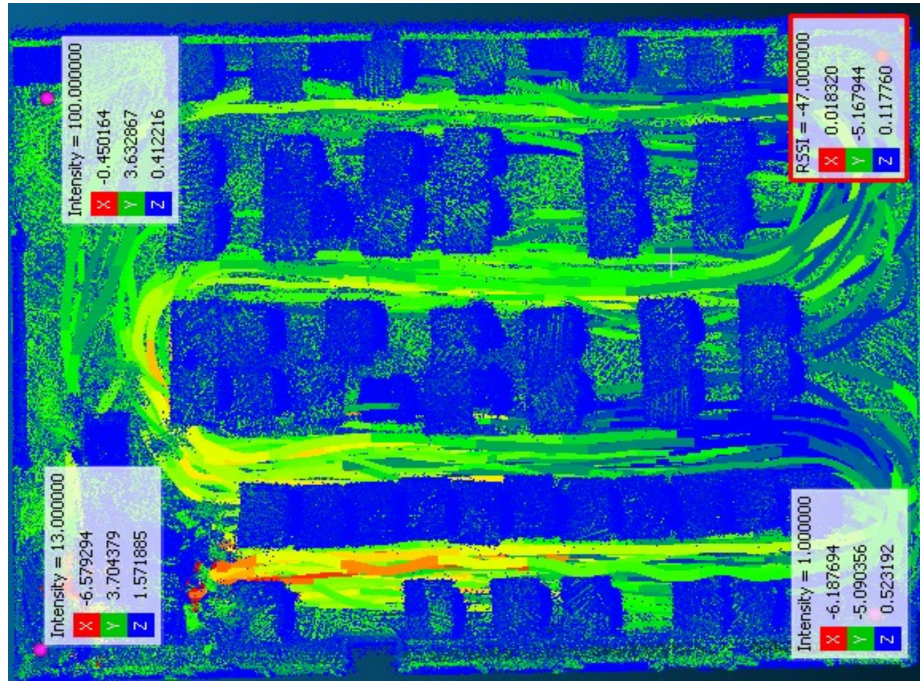


Figure 3.3: Cloudmap of room 7-611

3.3.3 RSSI Value Measurement

The Raspberry Pi (RPi) is a compact single-board computer birthed by the Raspberry Pi Foundation. While its initial intention was to foster computer science education, its adaptability soon found it embedded in a myriad of tech ventures. The RPi, equipped with ARM CPUs, GPIO pins, USB ports, and supporting multiple operating systems, most notably Raspbian, has become a staple for hobbyists and professionals alike, especially in the realms of embedded systems and IoT applications. For our specific project involving the Emesent Hovermap, we harnessed the capabilities of the RPi. We mounted the RPi

module on the Hovermap as shown in the Figure3.4, capitalizing on its integrated Wi-Fi module to systematically capture the received signal strength indicator (RSSI) values— a widely acknowledged metric to gauge the connection quality in wireless systems like Wi-Fi, Bluetooth, and cellular networks. These RSSI values, articulated in decibel-milliwatts (dBm), after collection, underwent preprocessing to discard NaN values and anomalies. To ensure seamless integration of data, the location particulars derived from the Emesent Hovermap and the RSSI figures captured by the Raspberry Pi were synchronized through Python-based timestamp alignment.

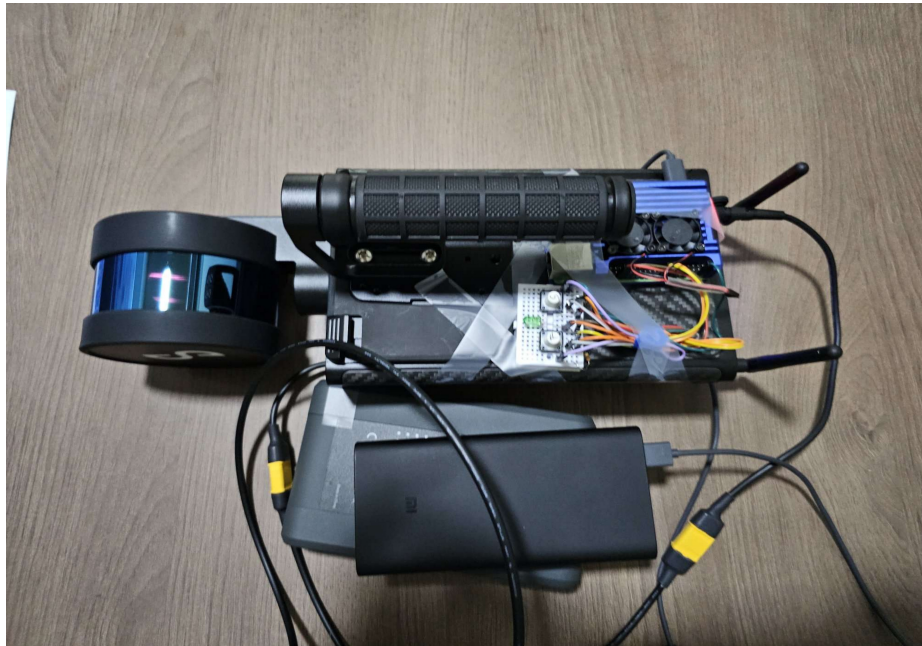


Figure 3.4: Raspberry Pi mounted on EMESENT Hovermap

In our experimental framework, we engaged 16 distinct clients for model updating. Each client traversed ten specific paths, updating the model at every juncture. For instance, the eight paths taken by client 1 during its model updates are depicted in Figure ?? . It's worth noting that every client adopted diverse paths for data collection in each instance. The newly acquired data was then employed by each client to train its local model, ensuring

compliance with predetermined model guidelines and hyperparameters. After the local training, the model weights were relayed to a centralized server. Here, these weights underwent aggregation to refresh the global model’s parameters. This cyclical procedure, alternating between individual training and centralized weight aggregation, was systematically performed for all 16 clients across ten communication cycles.

3.4 System Model

Traditional centralized learning methodologies generally comprise three stages: 1) data preprocessing, 2) data consolidation, and 3) model creation. In the context of centralized learning, data preprocessing implies deriving data features and labels from raw data forms, such as text, imagery, and application-specific data, prior to engaging in data consolidation. This stage incorporates substeps like sample acquisition, outlier elimination, feature normalization, and feature amalgamation. With respect to data consolidation, traditional learning models invariably partake in direct data exchanges amongst parties to secure a comprehensive database for training purposes. This approach, however, confronts the emerging hurdles of data privacy laws and regulations because institutions risk privacy breaches and infringement of legal frameworks such as the General Data Protection Regulations (GDPR) through such data sharing procedures. FL is proposed as a solution to the aforementioned issues. Nevertheless, extant FL frameworks frequently resort to rudimentary ML models such as XGBoost and decision trees instead of complex deep learning models [46]. These models necessitate uploading copious parameters to the cloud within the FL framework, culminating in substantial communications overhead, which may precipitate training failures for individual or global models. Consequently, FL frameworks require the

establishment of a novel parameter consolidation mechanism for deep learning models to attenuate communications overhead.

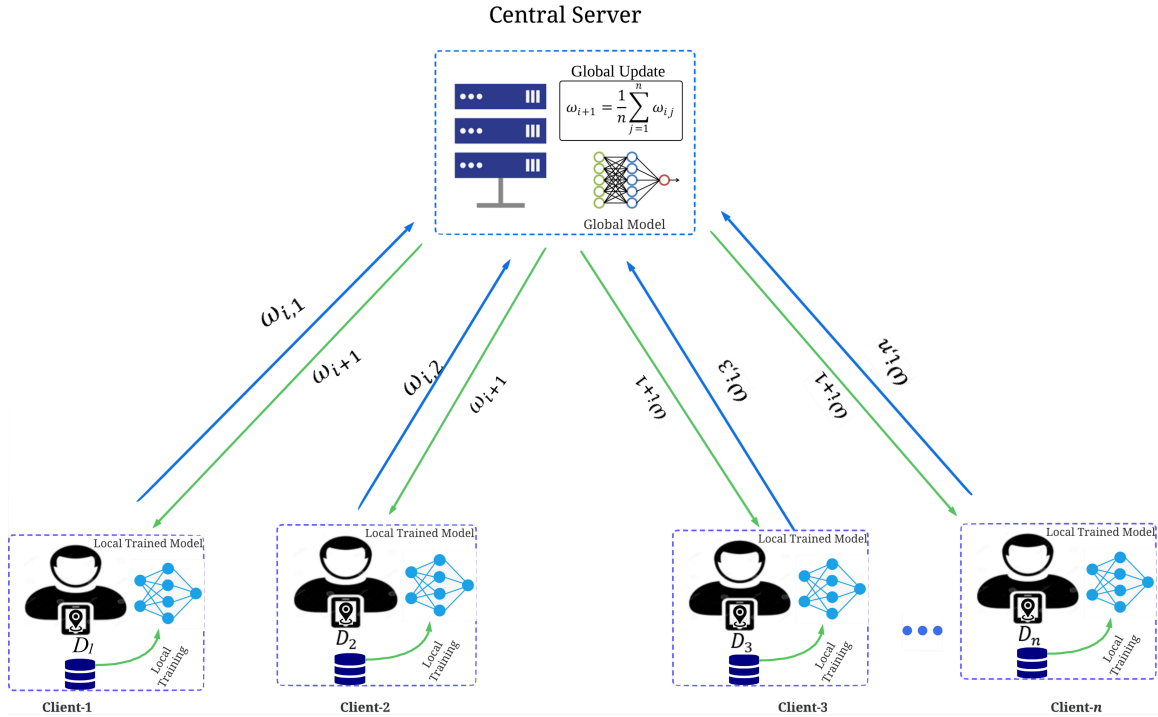


Figure 3.5: Federated learning overview

It is noteworthy to highlight the FL approach's security potential. In contrast to traditional methods that may violate privacy laws like GDPR, FL ensures that raw data remain at the source, drastically reducing the likelihood of data breaches. It instead deals with model parameter updates, which do not contain sensitive information and are difficult to reverse-engineer. Thus, FL provides a layer of protection that is crucial in today's increasingly privacy-conscious world.

3.4.1 Federated Learning

FL is a novel approach to ML where a model is trained across multiple devices or servers while keeping the data localized. Instead of transferring raw data to a central

server for training, FL pushes the model to edge devices (smartphones, tablets, IoT devices, etc.) and allows training to happen locally on each device. After local training, only the model updates are sent to the central server where they are aggregated and the global model is updated. Figure 3.5 shows the overall FL process. This approach addresses multiple concerns, such as privacy, security, and data ownership, while ensuring a quality model.

In the context of wireless communications, consider a system with N clients where each client, j , has its own distinct local dataset. The FL procedure begins with the central server initializing the global model. Let the parameters of this model be denoted by ω . For the i^{th} iteration of the FL process, the central server shares the current global model parameters, ω_i , with all N clients. Subsequently, each client j utilizes its dataset to conduct local training. Through this, it computes an updated version of the model parameter, which we label $\omega_{i,j}$. After completion of this local training phase, each client's updates are sent back to the central server. The server then aggregates these updates using Federated Averaging (FedAvg) shown in Algorithm 1. The aggregated update for the i^{th} iteration is described by the following equation:

$$\omega_{i+1} = \frac{1}{n} \sum_{j=1}^N \omega_{i,j} \quad (3.1)$$

This signifies the averaging of all local model parameters to yield the global model parameter for the subsequent iteration. The major advantages of FL in the context of wireless communications include preserving the privacy of user data, reducing the communications load from transmitting large datasets, and harnessing distributed data resources.

3.4.2 FedLSTM Architecture

LSTM is a specialized type of recurrent neural network (RNN) designed to remember and utilize information over extended sequences. This capability addresses the vanishing

Algorithm 1 Federated Learning Process with FedAveraging

```

1: Initialize global model parameters  $\omega$  on central server
2: for round = 1 to  $i$  do                                     ▷ Repeat for  $i$  communication
   rounds
3:   selected_clients  $\leftarrow$  Randomly select  $N$  clients
4:   for each client  $j$  in selected_clients do
5:     Send current model parameters  $\omega_i$  to client  $j$ 
6:      $\omega_{i,j} \leftarrow$  client  $j$  performs local training using its
       data
7:     Send  $\omega_{i,j}$  back to central server
8:   end for
9:    $\omega_{i+1} \leftarrow 0$ 
10:  for each client  $j$  in selected_clients do
11:     $\omega_{i+1} = \omega_{i+1} + \omega_{i,j}$ 
12:  end for
13:  Apply FedAvg:
14:   $\omega_{i+1} = \omega_{i+1} / N$                                      ▷ Average the updates
15:  Send updated model parameters  $\omega_{i+1}$  to all
       selected_clients
16: end for

```

gradient problem commonly observed in traditional RNNs, enabling LSTM to learn and retain long-term dependencies in the data. Often utilized in time series prediction and other sequential tasks, LSTM significantly improves the efficiency and accuracy of deep learning models dealing with sequential data. RSSI prediction based on x and y geographic coordinates, can be done by the LSTM model. We train the LSTM model in a federated manner at the edge, and update the global model on the server. This proposed federated LSTM is called FedLSTM owing to the nature of its training. At first, the global model is initialized with random weights, and is then updated by the clients locally. The layer architecture starts with an LSTM layer of 256 units, designed to process spatial input and extract pertinent sequential patterns. To avoid overfitting, a subsequent dropout layer is employed, ensuring the model remains generalizable across diverse radio conditions. The succeeding layers (LSTM with 128 units and 64 units) progressively refine these patterns with intermittent dropout layers for regularization. The architecture ends with a pair of dense layers; the first handles the processed data, and the subsequent layer outputs the predicted RSSI value. The detailed, layer-by-layer architecture is described in Table 3.1.

What sets this research apart is its innovative adoption of federated learning. Rather than centralized model training, the architecture is distributed across multiple clients. Each client refines the model using local data before sending weight updates to a central server. This decentralized approach not only accentuates data privacy but also captures the diverse radio environments each client is exposed to, ensuring a more comprehensive and applicable real-world REM.

3.4.3 REM Construction

In this subsection, our primary focus is the construction of a deep FL model designed to predict indoor propagation coverage for Wi-Fi networks using x and y coordinates of the

Table 3.1: Architecture of the LSTM Network

Layer (type)	Output Shape	Param #	Description
lstm_3 (LSTM)	(None, 3, 256)	265,216	LSTM layer
dropout_3 (Dropout)	(None, 3, 256)	0	Regularization layer
lstm_4 (LSTM)	(None, 3, 128)	197,120	LSTM layer
dropout_4 (Dropout)	(None, 3, 128)	0	Regularization layer
lstm_5 (LSTM)	(None, 64)	49,408	LSTM layer
dropout_5 (Dropout)	(None, 64)	0	Regularization layer
dense_2 (Dense)	(None, 32)	2,080	Fully connected layer
dense_3 (Dense)	(None, 1)	33	Fully connected layer
Total Parameters: 513,857			
Trainable Parameters: 513,857			
Non-Trainable Parameters: 0			

area of interest. To design the deployment model, we trained the deep FedLSTM network in a distributed manner. This can be mathematically represented as

$$\mathcal{L}(\theta) = \sum_{j=1}^N w_j \mathcal{L}_j(\theta) \quad (3.2)$$

where $\mathcal{L}(\theta)$ denotes the global loss function, N is the total number of local datasets, w_j signifies the weight assigned to each local dataset, and $\mathcal{L}_j(\theta)$ represents the loss function for the j^{th} local dataset.

The input dataset, denoted \mathcal{D} , is partitioned into two subsets: $\mathcal{D}_{\text{train}}$ (for training) and $\mathcal{D}_{\text{valid}}$ (for validation or testing). This division is crucial for effective hyperparameter tuning. As a result, parameters θ are fine-tuned based on evaluation metrics such as relative error ϵ , MAE, RMSE, and R^2 scores.

To visualize the radio map over our target area, we constructed a mesh grid with 1000×1000 points. This grid was delineated by considering the minimum and maximum coordinates within our region of interest. To achieve this, we employed the Emesent Hovermap, which utilizes a LiDAR sensor in tandem with SLAM to produce a 3D representation of the environment. The resulting data are processed in CloudCompare, producing a point cloud. This point cloud can be further refined into a comprehensive 3D model, such as a mesh derived from the identified extreme points.

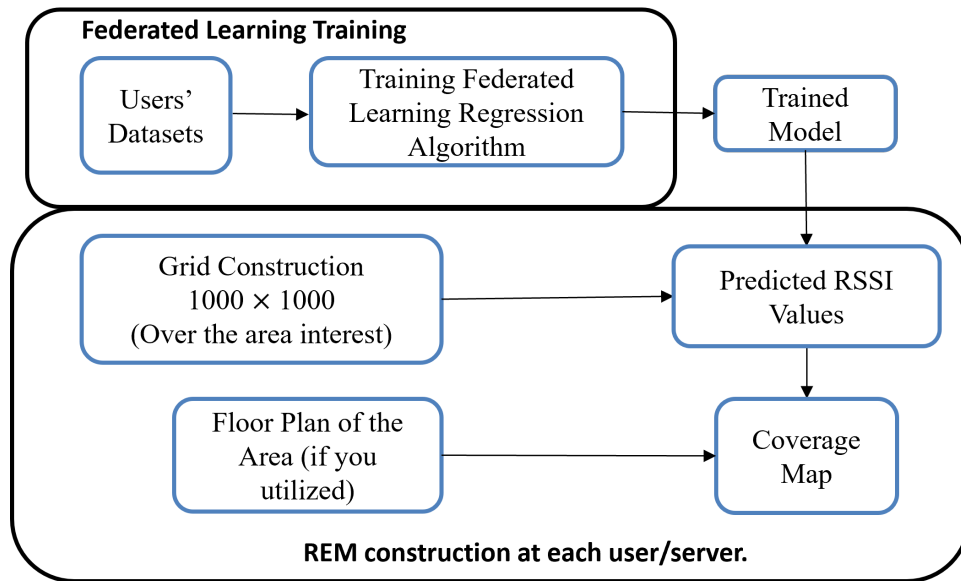


Figure 3.6: REM Construction.

Subsequent steps involve feature normalization based on the Z-score. We then employ a FedLSTM-driven regression approach tailored for the prediction task. Using the model trained in a federated manner, coverage predictions are determined from the RSSI values for each grid point. The predicted values derived from the federated framework are then combined with horizontal and vertical coordinates of the grid. This results in a REM visualizing the predicted data points as a pseudocolor plot, which is rendered into a 2D map using the pcolor function. Complementing this, a bar graph is introduced to correlate our data with the associated color representation in each plot. For a clearer understanding, Figure 3.6 provides a detailed graphical representation of the entire procedure.

Fine Tuning Process

For construction of the REM, the fine-tuning procedure necessitates systematic optimization of various hyperparameters to achieve optimal model performance. Determining the optimal network architecture, including the choice of layers, is critical. Additionally, regularization parameters are carefully adjusted to prevent overfitting and improve the model's generalization capability. Time steps, which influence LSTM's ability to capture temporal dependencies, are also an essential aspect of this fine-tuning. The entire optimization process is carried out on a trial-and-error basis. The performance of each configuration is assessed using several metrics, namely RMSE, R^2 score, and relative error. Each iteration provides insights, helping subsequent adjustments to refine the model's performance for REM construction. The detailed fine-tuning process is illustrated in Figure 3.7.

3.4.4 Model Evaluation

In this subsection, we evaluate the efficiency of the proposed federated model with different evaluation error metrics: RMSE, MAE, relative error, R^2 score, and mean

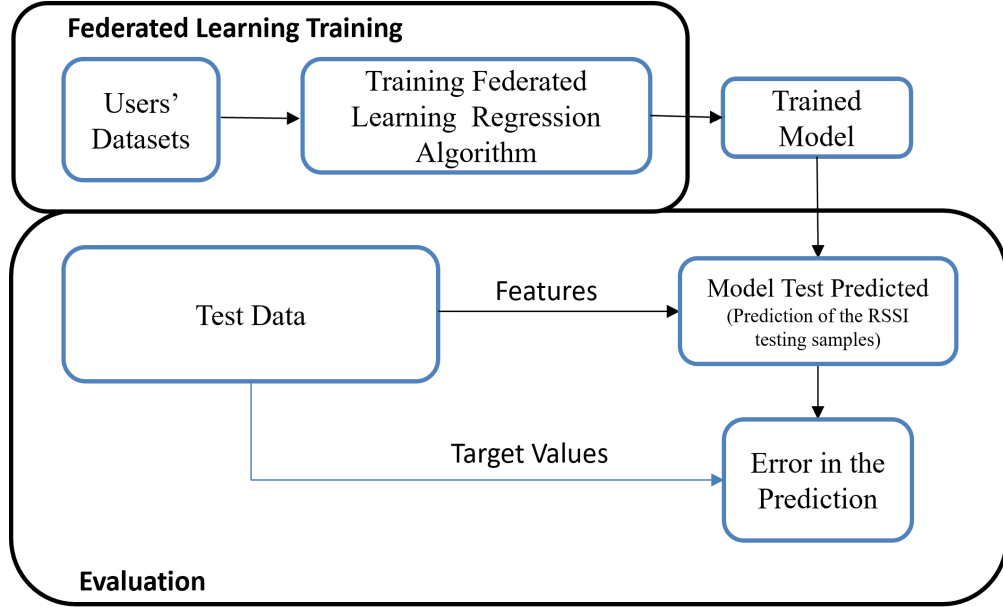


Figure 3.7: Fine-tuning the FedLSTM network for REM construction.

absolute percentage error (MAPE). These error metrics can best evaluate the performance of the model in different ways. In the field of wireless communications, they play a vital role in evaluating the performance of the prediction model. Predicting RSSI at distinct x and y coordinates demands a comprehensive understanding of the deviations between true measurements and predicted values, because these can greatly influence the precision of REM generation. Recognizing these error metrics aids in refining and bolstering predictive models. Some of the main metrics are explained below.

Root Mean Square Error shows the average squared deviations between true values, y , and predicted values, \hat{y} . In REM building, a low RMSE means the federated LSTM model predicts RSSI values accurately across different locations. The formula for RMSE is

$$Er_{RMSE} = \sqrt{\frac{1}{m} \sum_{i=1}^m (y_i - \hat{y}_i)^2} \quad (3.3)$$

Mean Absolute Error calculates the average deviation between predicted and true values. This metric becomes essential in scenarios where accurate RSSI predictions are critical for precise REM construction:

$$Er_{MAE} = \frac{1}{m} \sum_{i=1}^m |y_i - \hat{y}_i| \quad (3.4)$$

Relative Error provides a deviation measure adjusted by the actual value. Considering the diverse range of wireless signal strengths, this metric evaluates the proportional differences between predicted and actual values across various signal levels:

$$Er_{Relative} = \frac{|\hat{y}_i - y_i|}{y_i} \quad (3.5)$$

Mean Absolute Percentage Error characterizes the deviations of predictions in terms of their percentage errors from actual observations. Given its foundation in relative accuracy, MAPE is paramount for discerning the fidelity of REM predictions in the context of empirical data:

$$Er_{MAPE} = \frac{100}{m} \sum_{i=1}^m \left| \frac{y_i - \hat{y}_i}{y_i} \right| \quad (3.6)$$

The R^2 **score**, also known as the coefficient of determination, measures how well the model's predictions correspond to the actual data. An R^2 value approaching 1 indicates the model accounts for most of the variability in the data, signifying precise RSSI predictions suitable for REM creation. Conversely, an R^2 value approaching 0 suggests the predictions are predominantly aligned with the data's average, potentially lacking in genuine predictive power:

$$Er_{R^2} = 1 - \frac{\sum_{i=1}^m (y_i - \hat{y}_i)^2}{\sum_{i=1}^m (y_i - \bar{y}_i)^2}, \quad (3.7)$$

with \bar{y}_i representing the mean target value.

Overall, these metrics address various dimensions of prediction accuracy. By analyzing them collectively, we obtain a comprehensive understanding of the model’s performance and robustness, which is critical for optimal wireless communications and precise REM generation.

Implementation Platform

We utilized the NVIDIA GeForce RTX 3060 Graphics Processing Unit (GPU) for our training processes. This GPU enables us to undertake sophisticated deep-learning tasks with remarkable efficiency and speed. The NVIDIA GeForce RTX 3060 is equipped with a state-of-the-art Ampere architecture boasting 3584 CUDA cores capable of delivering impressive computational throughput. Alongside this, the card is complemented with 12 GB of GDDR6 memory, ensuring swift data handling during intensive operations. For our development environment, we utilized Python, and structured our deep learning architectures using the TensorFlow framework.

3.5 Numerical Results

In this section, we evaluate the performance of the proposed FL model using various testing scenarios. We established multiple experimental setups to rigorously analyze the behavior of the FedLSTM network under different conditions. Initially, the REM was constructed using a centralized LSTM network with a consistent architecture. This served as a baseline to compare against the federated configuration of the REM employing the same architecture. We conducted evaluations of FedLSTM based on different numbers of clients in the training process, enabling an assessment of performance fluctuations. The effect of varying local epochs on client devices was also studied to evaluate the adaptability of less computationally robust devices. Additionally, FedLSTM’s performance was examined across

different client configurations and batch sizes, elucidating their respective impacts on model efficiency. Detailed numerical results of these evaluations are provided in the subsequent subsections.

3.5.1 Comparison with a Centralized LSTM Network

To evaluate our federated model’s performance, it is essential to compare it against a centralized model. In our experiment, we employed a federated setup consisting of 10 clients. Each client moved along a different path to collect data from different parts of the area of interest. The model was created on the main server and then distributed to the participating clients. After each client trains the model using their data for these two rounds, the updates are sent to the central server. The server integrates each update with those from other clients, and then relays the consolidated model to another randomly chosen client. For this experiment, data processing was conducted in batch sizes of 32. Referring to the results in Figure 3.8, our Federated LSTM model’s performance metrics (RMSE, MAE, and R^2 score) were assessed against the centralized model.

The federated model’s RMSE was marginally elevated by 0.1 dBm in comparison to its centralized counterpart. The MAE metric indicated a prediction difference of approximately 0.2 dBm. When evaluating the R^2 score, the centralized model exhibited a slight advantage. However, it is crucial to highlight that while the centralized model offers marginally better performance, it raises concerns over data privacy, demands higher computational resources, and creates more communications overhead. Particularly in the process of aggregating data across an expansive geographic spectrum for REM construction, the centralized methodology demands substantial bandwidth for data transmission, which is a concern for participants reluctant to disclose their location due to potential security and privacy breaches.

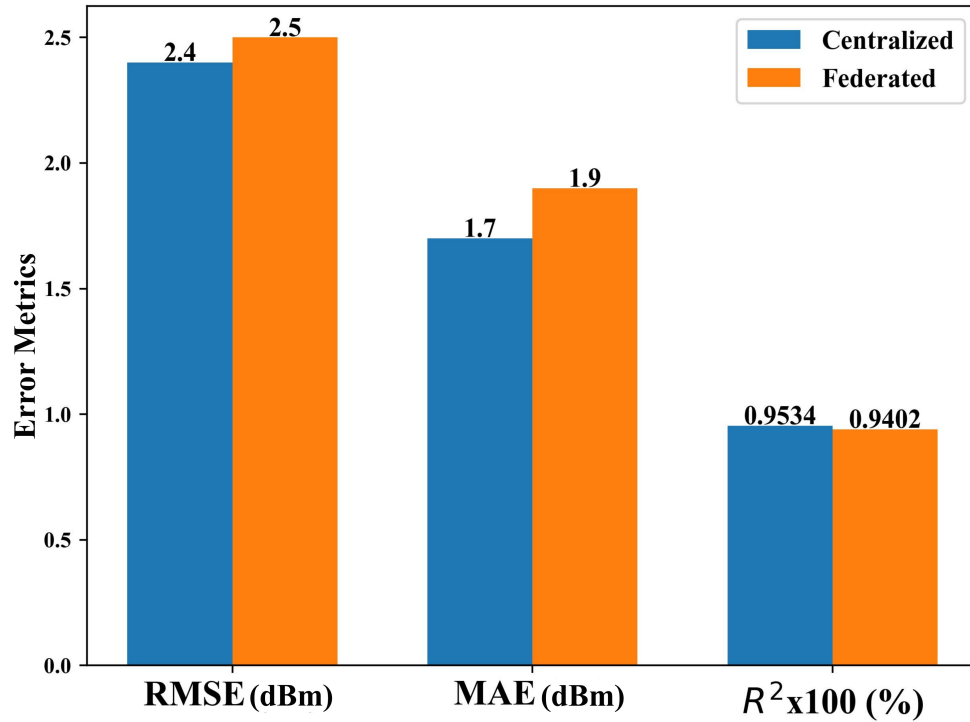


Figure 3.8: Performance Comparison of centralized and federated LSTM networks

3.5.2 Impact of the Number of Clients on Global Convergence

In this assessment, we evaluate the impact of the number of clients participating in convergence of the federated model. The model was employed in different federated settings; each time, the number of participating clients was changed to observe the behavior of the model. We evaluated the regression model with five error metrics, namely, RMSE, MAE, R^2 , relative error, and MAPE. In general, the performance of the model can attain the expected efficiency with various numbers of clients participating in the FL model. However, the more clients, the sooner the system will converge to the global minimum.

Therefore, with a large number of clients using FedLSTM, prediction accuracy can quickly achieve high performance, and thus, the accuracy will be more stable through communication rounds. Figure 3.9 shows that for $C = 16$, the R^2 score of the FedLSTM

model reached 90% after just two communication rounds, and reached 93% after 10 rounds. In contrast, the system with few assigned clients ($C = 4$) had a relatively lower R^2 score, not going above 90% even after 10 communication rounds.

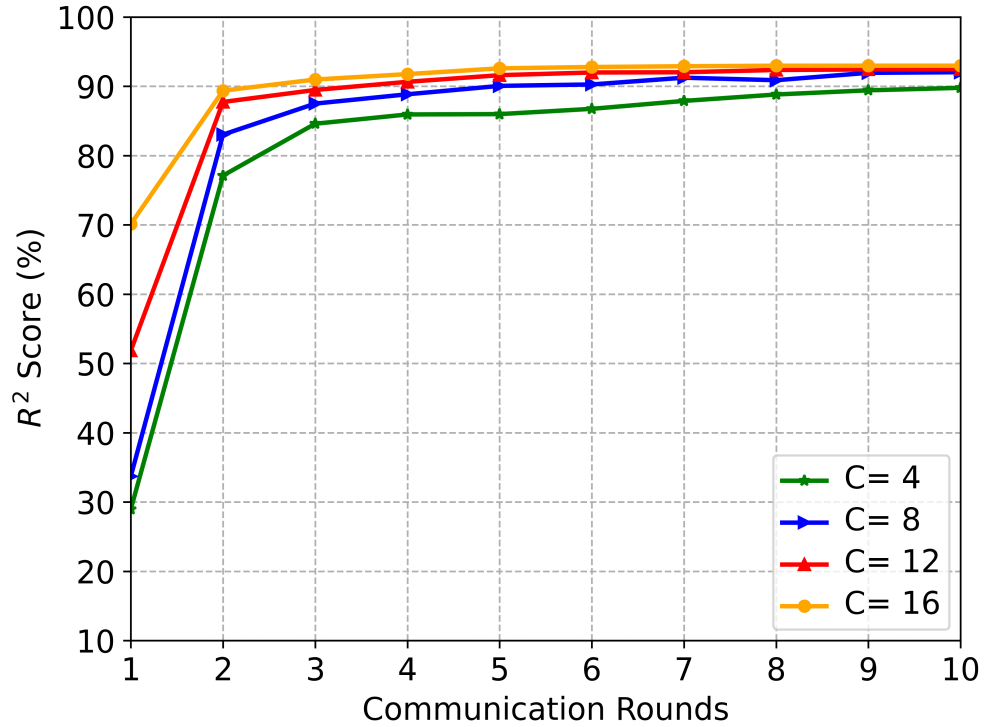


Figure 3.9: R^2 variations from the number of clients

Similarly, Figure 3.10 shows that the RMSE of the federated model also showed a lower value, which means best performance, when the number of clients in model training was high ($C = 16$). The proposed federated model showed a lower RMSE in all communication rounds when C was 16. This error metric was high when C was 4. In the early communication rounds, the model with four clients showed fast convergence. However, convergence was reduced after five communication rounds. This means that with fewer clients, the model may start with sharp convergence, but it may stop further along with certain communication

updates.

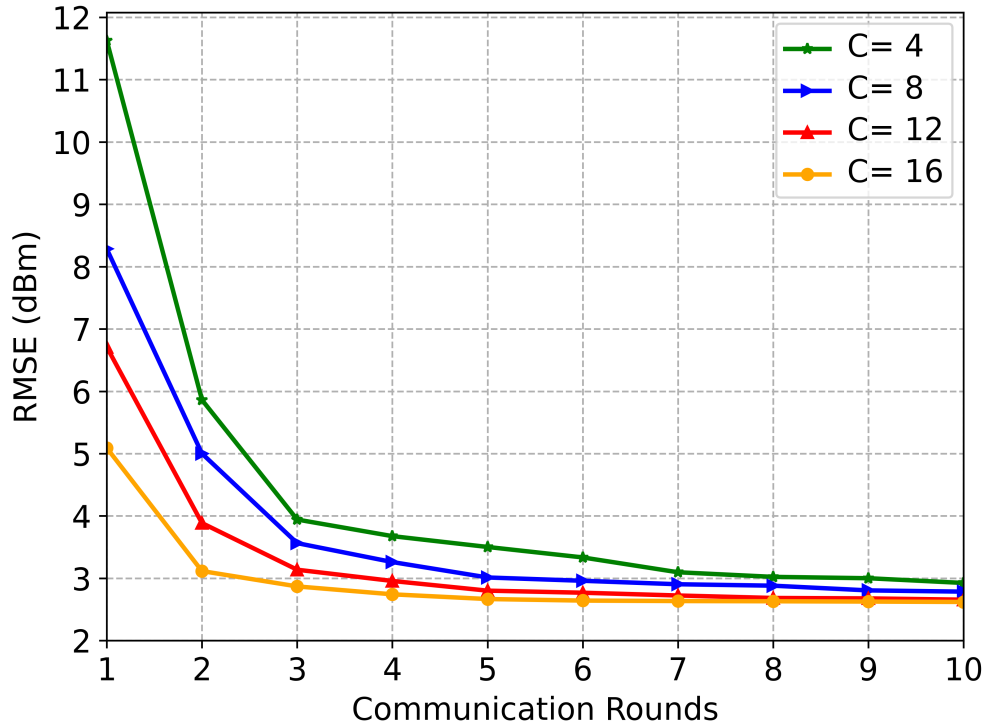


Figure 3.10: RMSE variations from the number of clients

In addition, MAE calculates the average deviation between predicted and true values, and in our setting, MAE also followed the trends in Figure 3.11. The graph depicts high MAE in every communication round when $C = 4$. Even after 10 rounds, MAE was 3 dBm, just above 2 dBm when clients numbered 8 and 12. However, MAE decreased continuously to 2 dBm after eight communication rounds, and the trend continued, decreasing to below 2 after 10 rounds.

Furthermore, the model was evaluated with relative error to show the deviations from actual values and the proportional differences between predicted and actual values

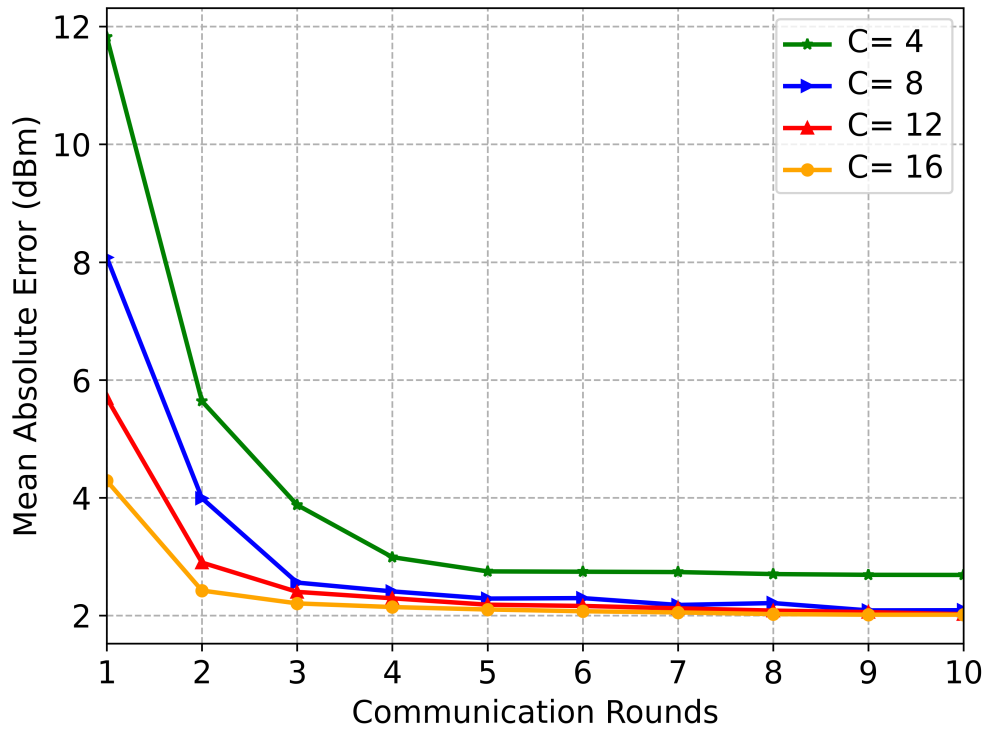


Figure 3.11: MAE variations from the number of clients

across the data. The relative error graph in Figure 3.12 illustrates that an increase in clients had a strong impact. Relative error was above 0.06 dBm before five communication rounds had been completed, and then dropped to about 0.05 dBm after 10 rounds. This error metric followed the same trend as metrics discussed above, meaning that relative error decreased with each client added to train and update the model. This error was near 0.03 dBm when $C = 16$ after 10 rounds for updating the model. With that many clients, the error dropped very fast in the beginning as well.

Finally, to characterize deviations in predictions in terms of percentage errors from actual values the mean absolute percentage error was evaluated based on variations in the number of clients updating the model.

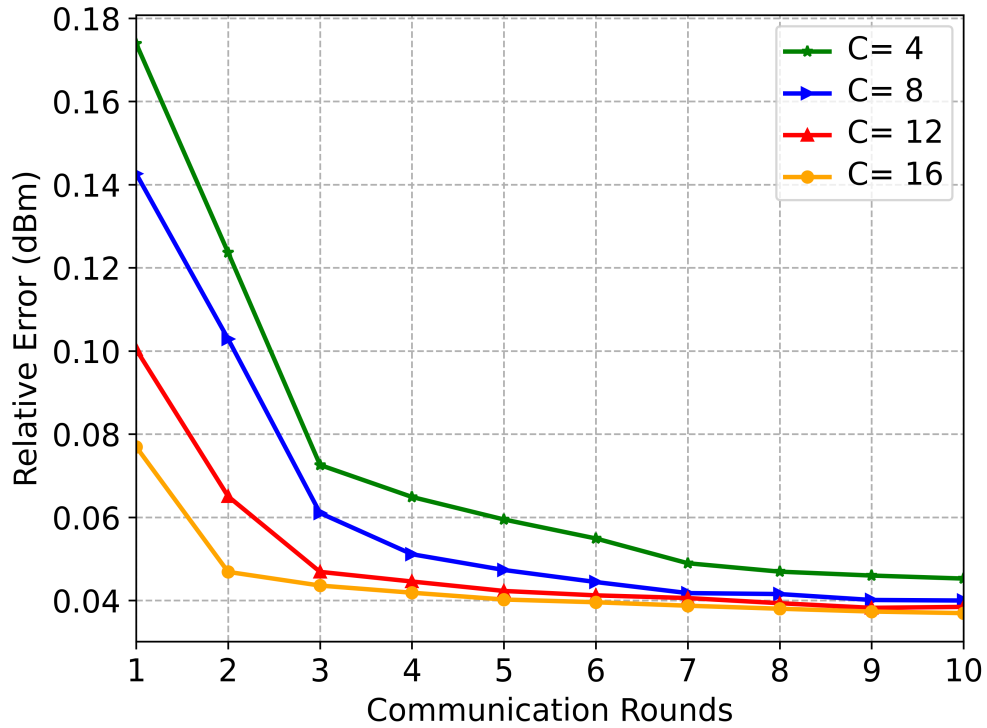


Figure 3.12: Relative error based on the number of clients

Figure 3.13 shows MAPE was below 4% when $C = 16$ after 10 rounds. In contrast, this error increased to around 5% when $C = 4$. MAPE was around 4% with eight and 12 clients, but converged to these values in the final updates, compared with 16 clients updating model weights.

Overall, for a system with 16 clients, in comparison with the four-client system, accuracy and precision were higher with notably fewer errors. Generally, in a predetermined number of training rounds, the number of clients affects the FL process accuracy and convergence speed. As more clients participated in the FL process in each round, the model's absolute precision and training speed suffered from fewer adverse effects. Nevertheless, once C improved to a particular level, advancement of system performance was less noteworthy, and sometimes even degraded. When putting the FL process into practice, we can face

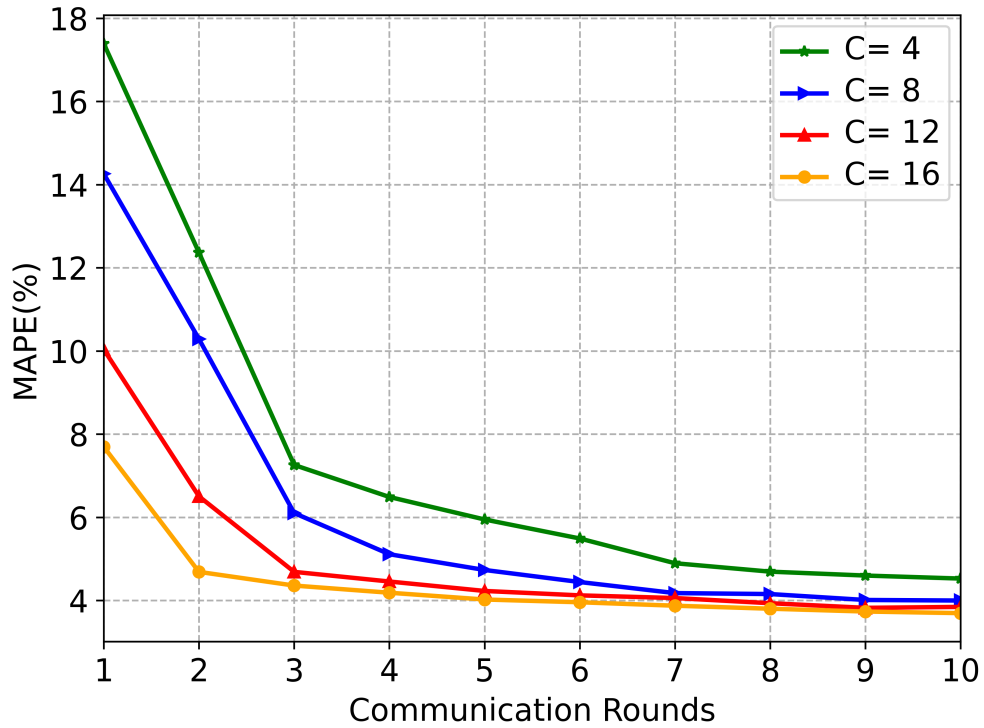


Figure 3.13: MAPE variations based on the number of clients

difficulties in that as C increases, more clients update local parameters to the server. As a consequence, the communication and computation costs of the FL model amplify significantly. This is encouraging because, in real-world applications with large-scale clients, we only need to select a set of clients from the network to execute the FL process in each communication round. This procedure saves considerable communication costs in the FL process.

3.5.3 Contribution of Local Model Epochs to Global Convergence

In ML, an epoch is one complete cycle through the full training dataset. Specifically, each epoch involves both forward propagation (estimation of output given the input) and backward propagation (adjustment of model weight based on error). The number of epochs is a hyperparameter that determines how many times the learning algorithm will work

through the entire training dataset. In the context of FL, where data remain distributed across multiple devices or nodes and do not converge centrally, the local number of epochs becomes a pivotal factor. It dictates how much training is conducted on each local dataset before aggregating model updates into the global model. This subsection delves into the nuanced influence that varying the local number of epochs has on convergence speed and quality in FL setups.

From Figure 3.14, it is evident that as the number of epochs for training on each selected client per communication round increased, the RMSE of the federated model decreased. To elucidate, in the federated setting where the number of epochs was set to two ($\epsilon = 2$), the model experienced rapid convergence initially but plateaued at a value of 2.75 dBm after 20 epochs. In contrast, as ϵ was incremented to 3, 4, and finally 5, the trends illustrate that the RMSE of the model with $\epsilon = 5$ remained consistently lower than the other three configurations in every communication round.

Similarly, to assess the accuracy with which our federated model represents the data, we evaluated the R^2 score. As depicted in Figure 3.15, our federated model achieves a commendable R^2 score of 93% after only a few communication updates when ϵ is set to 5. However, when the local epochs ϵ are adjusted to 4, 3, and 2, there is a subsequent decrease in the R^2 score for each setting. However, their impact on the global model convergence decreases with the increase in the number of communication rounds.

Furthermore, the model was assessed using relative error to demonstrate deviations, adjusted by the actual values, and to display the proportional differences between the predicted and actual values across the data. Figure 3.16 illustrates that as ϵ increased from 2 to 5, the FedLSTM model mirrored the trend exhibited by variations in the number of clients.

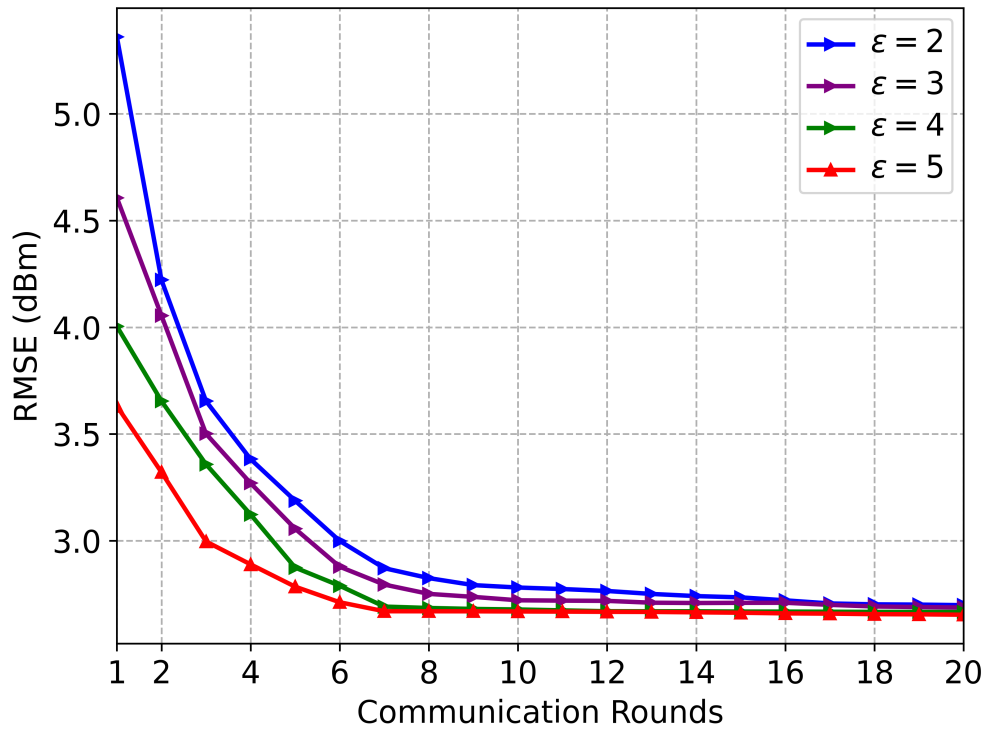


Figure 3.14: RMSE variations from the local number of epochs

In the initial communication rounds, ϵ significantly impacted global convergence. There appears to be a substantial difference between $\epsilon = 2$ and $\epsilon = 5$ in the early stages; however, after each update, this difference decreased to a certain extent. By the 20th communication round, the difference in relative error amongst the four settings for ϵ (5, 4, 3, and 2) was minimal, indicating that with more communication rounds, models with fewer or more epochs can exhibit nearly identical performance.

Figure 3.17 illustrates how MAPE, expressed as a percentage, quantified prediction deviations from actual error values based on variations in the number of clients during model updates.

Lastly, mean absolute error quantifies the average deviation between predicted and actual values. In our experiments, trends in MAE were consistent with those observed in

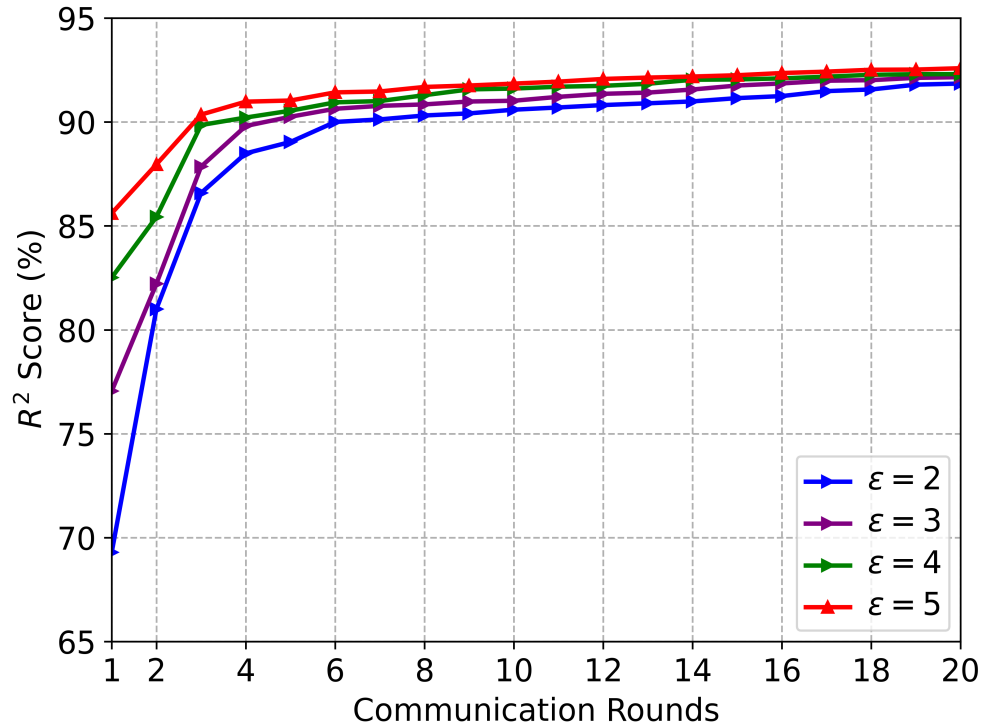


Figure 3.15: R^2 score variations based on the number of local epochs

other error metrics. Figure 3.18 illustrates how MAE was notably high during the initial communication rounds when $\epsilon = 2$. Conversely, when $\epsilon = 5$ for the first model aggregation, MAE was significantly lower. Yet as the aggregation rounds proceeded, the disparity in MAE between different ϵ settings diminished considerably, eventually converging to a value slightly above 2 dBm across all settings. Nonetheless, the model with $\epsilon = 5$ consistently registered a lower MAE, whereas $\epsilon = 2$ consistently exhibited a higher error value throughout the communication rounds.

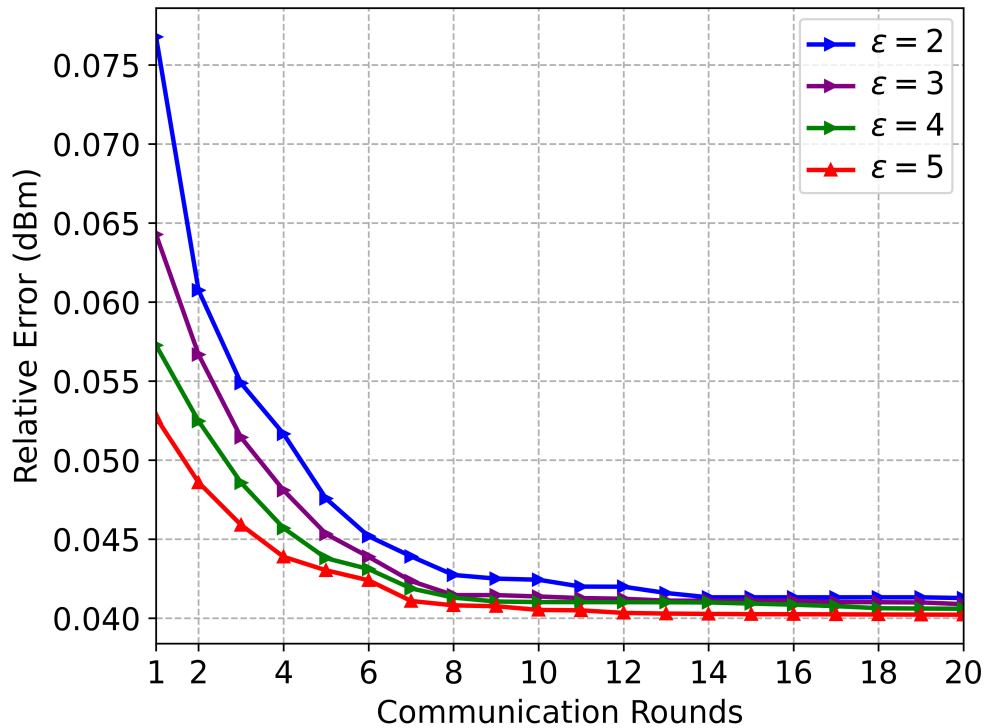


Figure 3.16: Variations in relative error based on the number of local epochs

3.6 Graphical Results

In the domain of wireless networking, the received signal strength indicator is a metric quantifying the signal power a device receives from the access point or router. Expressed in decibel milliwatts (dBm), RSSI is a pivotal criterion in evaluating the quality of a Wi-Fi connection. Under optimal wireless communications conditions, an RSSI value of -30 dBm represents peak signal reception. However, achieving such an ideal benchmark is infrequent in practical environments due to various interference and propagation factors. Signal strengths ranging from -50 to -30 dBm denote a very stable connection, facilitating seamless streaming and downloading. Between -60 and -50 dBm, the signal is still sufficiently strong for most standard applications, including uninterrupted streaming. However, as

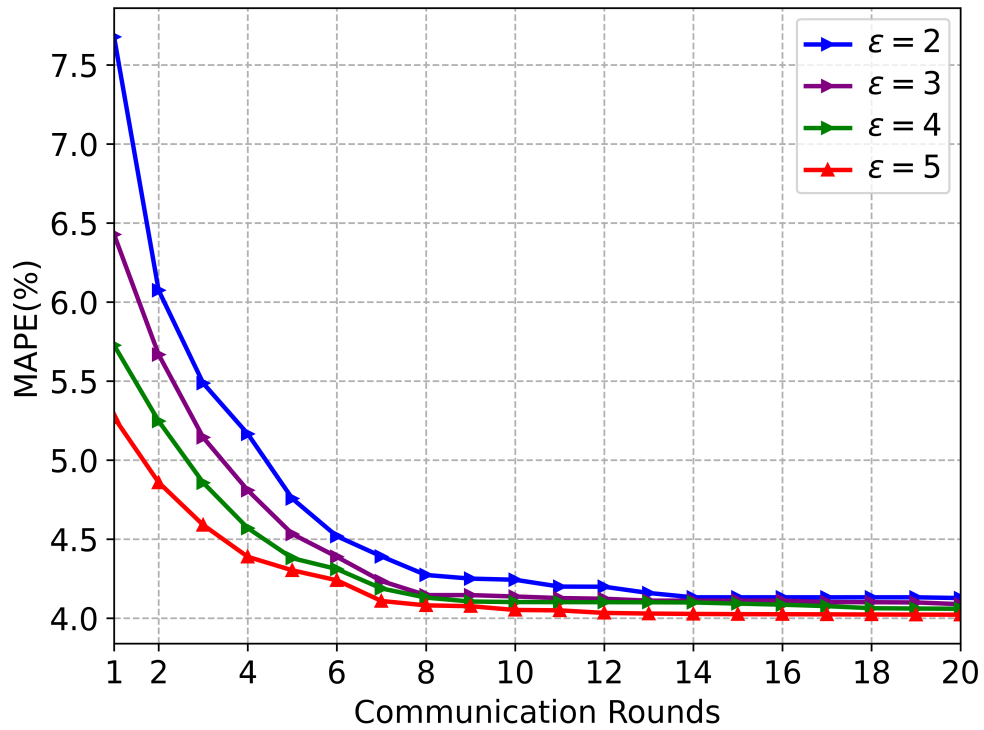


Figure 3.17: Variations in MAPE based on the number of local epochs

signal strength falls to the range of -70 to -60 dBm, performance becomes notably average. Connections in this range may struggle during intensive tasks, particularly if the network sees simultaneous activity from multiple devices or if the connected device is significantly mobile. Progressing further down the scale, a range of -80 to -70 dBm indicates an inconsistent connection prone to disruptions, especially during data-intensive operations like streaming. An even weaker range, -90 to -80 dBm, offers a highly unstable connection that is not only susceptible to frequent dropouts but also languid speeds. Any signal weaker than -90 dBm is practically non-functional, rendering a reliable connection almost impossible.

The dispersion of wireless signal strength is graphically represented as a 2D color map using the predicted RSSI values from the trained FL model. Figure 3.19(a) illustrates a LiDAR map of the area of interest constructed through the Emesent Hovermap, while

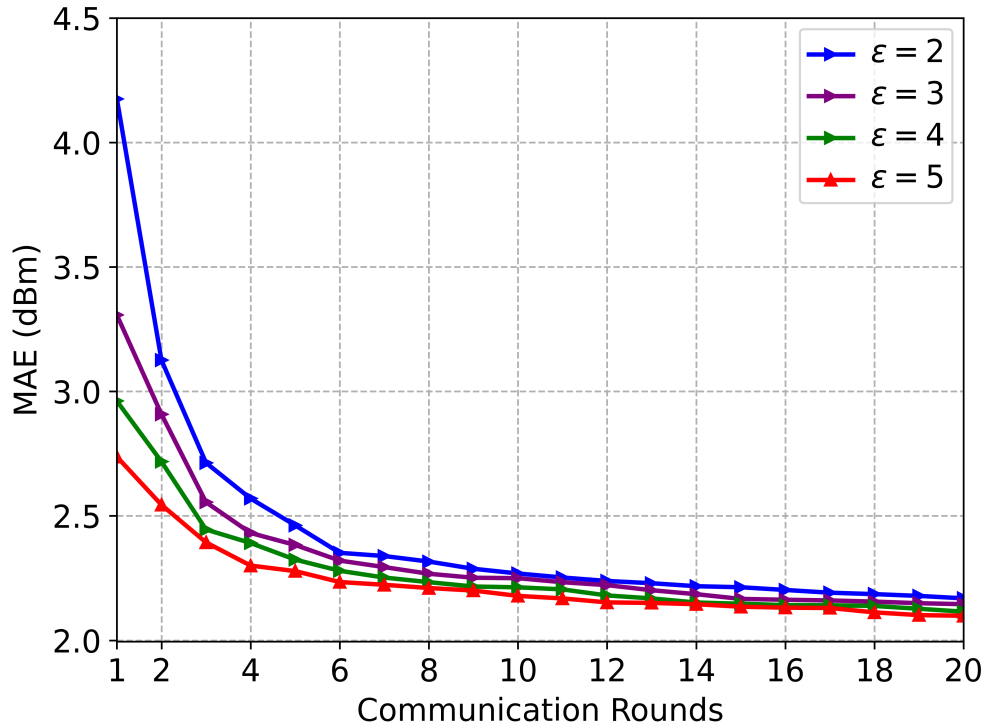


Figure 3.18: Variations in MAE based on the number of local epochs

Figure 3.19(b) displays the coverage map generated using the centralized LSTM model. In Figure 3.19(c), the REM constructed through the proposed FedLSTM model is presented. REMs constructed through the LSTM centralized model and FedLSTM are comparable, showing similar signal dispersion. Specifically, the region near the access point exhibits RSSI values above -50 dBm, indicating excellent signal strength. However, as one moves farther away from the access point, the RSSI values gradually decrease and eventually drop below -80 dBm at the far end of the area.

To further evaluate and test our proposed federated model under different settings, we conducted experiments inside a room. For this purpose, we utilized Room 7-611 at the University of Ulsan in South Korea. In this federated setting, we engaged five clients, each of which updated the model over 10 iterations for 10 communication rounds. Figure

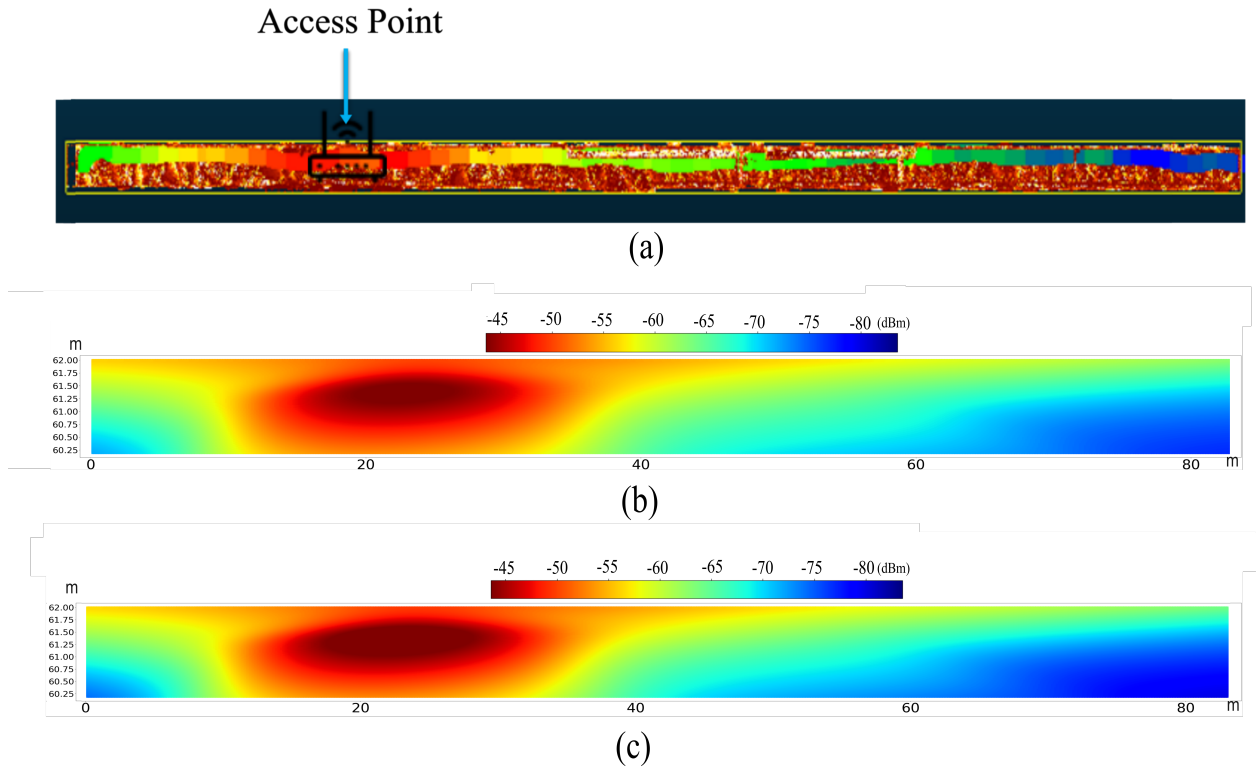


Figure 3.19: (a) Corridor layout, (b) REM from the centralized LSTM model, and (c) REM from FedLSTM

3.20(a) provides an overview of the room's layout, including an example path (*path_1*) followed by Client-1. In our scenario, we considered 10 paths taken by five clients. The centralized model's REM is Figure 3.20(b), and FedLSTM's REM in Figure 3.20(c) highlights the excellent coverage near the access point and the gradual reduction in signal strength when moving away from it. These graphic results demonstrate that in both room and corridor settings, FedLSTM achieved performance comparable to centralized approaches while concurrently ensuring data privacy, minimizing communications overhead, and reducing the server load.

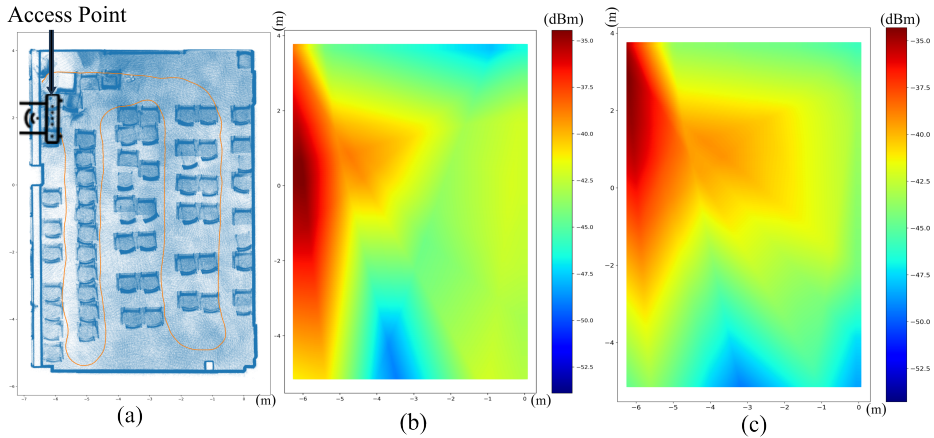


Figure 3.20: (a) Room layout, (b) REM from the centralized LSTM model, and (c) REM from FedLSTM

3.7 Conclusion

In this study, we presented an innovative approach called FedLSTM and based on FL for REM construction. In particular, the proposed FedLSTM framework is designed to predict indoor network coverage while addressing the pressing issue of data privacy. This proposed method is decentralized, allowing clients to participate in the training process without disclosing their data to a central server. For this approach, we utilized real measurements from various clients navigating different paths and updating their models with data from each path. When compared to a centralized counterpart, our model indicated a slight rise in RMSE to 2.5 dBm from 2.4 dBm and an increase in MAE to 1.9 dBm from 1.7 dBm. Subsequently, we evaluated the FedLSTM model considering variations in the number of participating clients. Numerical results revealed that increasing the number of clients enhanced performance metrics such as error rate and R^2 score. Additionally, adjusting

the number of local training epochs showed that even devices with limited computational power can meaningfully contribute to training the federated model, with fewer epochs still achieving competitive results. Graphic comparisons of REMs from FedLSTM and centralized LSTM highlighted their similarities. However, FedLSTM distinctly provided the trifold benefits of data security, communications efficiency, and a reduced server load. This research emphasizes FL's potential to ensure data privacy while upholding robust performance from indoor network coverage predictions.

Chapter 4

Summary of contributions and future works

4.1 Introduction

In the contemporary industrial landscape, the network infrastructures are undergoing significant evolutions, mirroring transformations observed in sectors like healthcare with the advent of e-health technologies. The pressing requirements of these modern industrial networks encompass enhanced capacity, rigorous security protocols, and cost-effective implementations. Our research offers an in-depth analysis of the integration of broadband Power Line Communication (PLC) and Wi-Fi technologies as a prospective solution to address these challenges. Utilizing the existing power line networks as foundational infrastructure, and supplementing them with cutting-edge Wi-Fi technologies, we highlight the instrumental capabilities of the Tenda PH10 AV1000 ACWI-FI POWER LINE ADAPTER in spearheading this integrative approach.

Through methodical experimentation, supplemented by realistic simulations and a

diverse set of test environments, we quantitatively and qualitatively assessed the advantages of merging PLC with Wi-Fi technologies. This hybrid approach not only augments the inherent capabilities of each individual technology but also represents a paradigm shift in the architectural design of industrial communication systems. The integration leads to substantial enhancements, such as uninterrupted data transmission, heightened operational efficiency, and the emergence of novel applications tailored for this combined technological platform. In a nutshell, this research not only provides empirical evidence of the immediate benefits derived from this integration but also delineates a roadmap for future research, anchoring the foundation for a seamlessly interconnected industrial ecosystem.

As we transition from the exploration of hybrid PLC and Wi-Fi frameworks to the domain of network design methodologies, it's paramount to recognize the interconnected nature of these innovations. The bedrock of a successful industrial network, as established, is contingent upon the blend of robust communication backbones and predictive intelligence. It's in this interstice that our subsequent investigations come into play. Just as the hybridization of PLC and Wi-Fi revolutionizes the tangible aspects of the network's infrastructure, the incorporation of federated learning paradigms redefines the abstract, data-driven mechanisms underpinning it. As industries evolve, so does the need for models that seamlessly intertwine the physical and the abstract, underscoring a holistic approach to network design and optimization. In the realm of industrial network design, the emphasis has traditionally been on centralized learning paradigms for network coverage prediction. However, with the digitization of contemporary industrial networks and the increasing complexities they present, there is a palpable need for more adaptive and privacy-preserving solutions. Our research introduces the Federated Learning-based Long Short-Term Memory (FedLSTM) model, a decentralized approach specifically tailored to address the emerging challenges of modern industrial settings.

Unlike its centralized predecessors, the FedLSTM model stands out by adeptly combining precision in prediction with a robust commitment to data privacy. Through extensive experimentation and data analysis, we've determined that the FedLSTM not only matches the benchmarks set by centralized models but, in many instances, surpasses them. It achieves this by leveraging the distributed nature of federated learning, thus optimizing communication pathways and equitably distributing server computational loads. Moreover, this decentralized approach underscores a critical advantage: the ability to train models without directly accessing user data, thus ensuring data privacy and reducing both communication overheads and server strain.

In essence, the FedLSTM model represents a pivotal advancement in network coverage prediction methodologies. It effectively responds to the evolving demands of the industrial landscape by offering a solution that balances accuracy, efficiency, and privacy. As industries continue their rapid digital transformation, the FedLSTM model, with its inherent advantages, is poised to become a cornerstone in future network optimization strategies.

4.2 Summary of Contributions

In this research dissertation, we conduct a comprehensive analysis of a hybrid network that integrates Power Line Communication (PLC) with Wi-Fi, proposed for modern industrial environments. To address the challenges associated with signal RSSI coverage prediction, a novel Federated Learning approach is introduced. The primary contributions of this thesis, in terms of advanced PLC-Wi-fi network optimization techniques and state-of-the-art coverage prediction methodologies, are outlined as follows:

- We developed an industrial setting using a hospital scenario as an example and analyzed the PLC-WiFi hybrid network in various environments by varying length of power line

cables.

- The existing industrial network was analyzed under practical scenarios. We connected an electrical load to the network and assessed the performance of the Tenda PLC slave, specifically focusing on its speed (in Mbps).
- After making the industrial network we introduce a new FL-driven method, FedLSTM, for predicting indoor coverage. FedLSTM allows for decentralized training by letting users forward only their model weights to the central server. This method differs greatly from traditional centralized systems that necessitate the transmission of both features and labels, resulting in increased data usage.
- We use Python software to build a REM, aiming to improve the visualization of coverage prediction. To achieve this, we create a data grid with 1000×1000 points within our target area, allowing us to display the coverage prediction on a 2D map.
- Our FL-based approach enables both the server and users to produce the REM. While the server acts as a network strategist, utilizing the REM to tackle coverage gaps by setting up access points or relays, users can evaluate their area's coverage and choose to move to regions with superior connectivity based on the REM insights.
- Furthermore, when contrasting the FedLSTM model with its centralized equivalent, our study highlights its security feature: only the model weights are relayed to the server, leaving the labels and features undisclosed. Such a methodology is especially beneficial in business, healthcare, and military environments where users are reluctant to divulge their location data to unidentified parties..

4.3 Future Direction

The primary focus of this dissertation is the efficient development of an industrial PLC-Wi-Fi hybrid network and the creation of a 2D radio map for the network's wireless component to optimize the network and enhance user experience. Additionally, this dissertation presents a federated learning approach to develop the Radio Environment Map (REM) using only the weights sent by each user to the server, instead of raw data. However, further research is needed to optimize the network and construct the REM.

- **Advanced Model Enhancements:** Delve deeper into the intricacies of federated learning architectures to identify potential areas of optimization and enhancement. An exploration into advanced topologies, as well as the incorporation of techniques such as model pruning, knowledge distillation, or attention mechanisms, may yield significant advancements. Moreover, an exhaustive study on LSTM networks, exploring bidirectional LSTMs, attention-based LSTMs, or hybrid LSTM architectures, can further improve the granularity and accuracy of predictions. It would also be prudent to consider methods for efficient weight aggregation in federated settings and the inclusion of robustness checks against potential adversarial attacks.
- **Scalability and Real-world Implementation:** Furthermore, a granular analysis considering various data distributions and heterogeneity across the nodes will offer insights into the model's robustness and adaptability. By emphasizing these technical dimensions, we aim to ensure that the FedLSTM model not only scales efficiently but also retains its performance efficacy in intricate industrial settings.
- **Security Protocols:** Since federated learning inherently emphasizes data privacy, further studies could dive deep into the cybersecurity aspects, ensuring that model

weights, when transferred, are secure from potential attacks. Also, a robust encryption technique is needed for federated learning in industrial settings.

- **Integration with IoT:** With the Internet of Things (IoT) becoming increasingly integral to industrial applications, examine how the hybrid PLC-Wi-Fi system can effectively communicate with a vast array of IoT devices, and investigate how the FedLSTM model can be fine-tuned to predict network behavior in an IoT-dense environment.

Publications

International Journal Papers

- [1] **Shafi Ullah Khan**, Noor Alam, Sana Ullah Jan, and In Soo Koo. “IoT-enabled vehicle speed monitoring system.” *Electronics*, 11, no. 4 (2022): 614.
- [2] **Shafi Ullah Khan**, Taewoong Hwang, and In Soo Koo. “Bridging the Connectivity Gap within a PLC and Wi-Fi Hybrid Network.” *The International Journal of Advanced Culture Technology*, 11, no. 1 (2023): 395-402.
- [3] **Shafi Ullah Khan**, San Ullah Jan, Taewoong Hwang, and In Soo Koo. “Efficient Hospital Indoor Communication Architecture for E-Health using Hybrid Wi-Fi and PLC Network: A Prototype” *Bulletin of Electrical Engineering and Informatics* .
- [4] **Shafi Ullah Khan**, Carla Garcia, Taewoong Hwang, and In Soo Koo. “Radio Environment Map Construction based on Privacy-centric Federated Learning” *IEEE Access*.

Journal Paper Excluded from Thesis

- [5] **Shafi Ullah Khan**, Sana Ullah Jan, and In Soo Koo. “Robust Epileptic Seizure Detection using LSTM and Feature Fusion from Compressed Time-Frequency EEG

Images” *Sensors*,

Bibliography

- [1] L. Sharma, “The rise of internet of things and smart cities,” *Towards Smart World: Homes to Cities using Internet of Things*, pp. 1–19, 2020.
- [2] P. Frehill, D. Chambers, and C. Rotariu, “A wireless network sensor and server architecture for legacy medical devices,” in *2008 International Conference on Telecommunications*, 2008, pp. 1–4.
- [3] D. Dietrich, D. Bruckner, G. Zucker, and P. Palensky, “Communication and computation in buildings: A short introduction and overview,” *IEEE Transactions on Industrial Electronics*, vol. 57, no. 11, pp. 3577–3584, 2010.
- [4] R. Kavitha, G. Nasira, and N. Nachamai, “Smart home systems using wireless sensor network—a comparative analysis,” *Int. J. Comput. Eng. Technol*, vol. 3, no. 3, pp. 94–103, 2012.
- [5] R. Sukanesh, S. Vijayprasath, P. Subathra *et al.*, “Gsm based ecg tele-alert system,” in *2010 International Conference on Innovative Computing Technologies (ICICT)*. IEEE, 2010, pp. 1–5.
- [6] N. Sriskanthan, F. Tan, and A. Karande, “Bluetooth based home automation system,” *Microprocessors and microsystems*, vol. 26, no. 6, pp. 281–289, 2002.

-
- [7] I. Poole, “What exactly is zigbee?” *Communications Engineer*, vol. 2, no. 4, pp. 44–45, 2004.
- [8] T. M. Fernández-Caramés, “An intelligent power outlet system for the smart home of the internet of things,” *International Journal of Distributed Sensor Networks*, vol. 11, no. 11, p. 214805, 2015.
- [9] P. Mlynek, M. Koutny, J. Misurec, and Z. Kolka, “Measurements and evaluation of plc modem with g3 and prime standards for street lighting control,” in *18th IEEE International Symposium on Power Line Communications and Its Applications*. IEEE, 2014, pp. 238–243.
- [10] G. Dickmann, “Digitalstrom®: A centralized plc topology for home automation and energy management,” in *2011 IEEE International Symposium on Power Line Communications and Its Applications*. IEEE, 2011, pp. 352–357.
- [11] P. Mlynek, Z. Hasirci, J. Misurec, and R. Fujdiak, “Analysis of channel transfer functions in power line communication system for smart metering and home area network,” *Advances in Electrical and Computer Engineering*, vol. 16, no. 4, pp. 51–56, 2016.
- [12] R. Kumar, S. Rani, and M. A. Awadh, “Exploring the application sphere of the internet of things in industry 4.0: a review, bibliometric and content analysis,” *Sensors*, vol. 22, no. 11, p. 4276, 2022.
- [13] C.-F. Chien, W.-T. Hung, and E. T.-Y. Liao, “Redefining monitoring rules for intelligent fault detection and classification via cnn transfer learning for smart manufacturing,” *IEEE Transactions on Semiconductor Manufacturing*, vol. 35, no. 2, pp. 158–165, 2022.

- [14] S.-F. Chou, H.-W. Yen, and A.-C. Pang, "A rem-enabled diagnostic framework in cellular-based iot networks," *IEEE Internet of Things Journal*, vol. 6, no. 3, pp. 5273–5284, 2019.
- [15] R. Dwivedi, D. Mehrotra, and S. Chandra, "Potential of internet of medical things (iomt) applications in building a smart healthcare system: A systematic review," *Journal of oral biology and craniofacial research*, vol. 12, no. 2, pp. 302–318, 2022.
- [16] F. Jamil, S. Ahmad, N. Iqbal, and D.-H. Kim, "Towards a remote monitoring of patient vital signs based on iot-based blockchain integrity management platforms in smart hospitals," *Sensors*, vol. 20, no. 8, p. 2195, 2020.
- [17] S. Razdan and S. Sharma, "Internet of medical things (iomt): Overview, emerging technologies, and case studies," *IETE technical review*, vol. 39, no. 4, pp. 775–788, 2022.
- [18] A. Winter, S. Stäubert, D. Ammon, S. Aiche, O. Beyan, V. Bischoff, P. Daumke, S. Decker, G. Funkat, J. Gewehr *et al.*, "Smart medical information technology for healthcare (smith) methods inf med. 2018 jul; 57 (s 01): e92–e105. doi: 10.3414," ME18-02-0004. <http://www.thieme-connect.com/DOI/DOI>, Tech. Rep.
- [19] C. Sridhathan and F. Samsuri, "Application of power line communication in healthcare for ecg and eeg monitoring," in *Proc. Of Int. Conf. on Advances in Power Electronics and Instrumentation Engeneering*, 2013.
- [20] Z. Fan, R. J. Haines, and P. Kulkarni, "M2m communications for e-health and smart grid: An industry and standard perspective," *IEEE Wireless Communications*, vol. 21, no. 1, pp. 62–69, 2014.
- [21] D. Dietrich, D. Bruckner, G. Zucker, and P. Palensky, "Communication and computation

- in buildings: A short introduction and overview,” *IEEE transactions on industrial electronics*, vol. 57, no. 11, pp. 3577–3584, 2010.
- [22] H. A. Alobaidy, M. J. Singh, M. Behjati, R. Nordin, and N. F. Abdullah, “Wireless transmissions, propagation and channel modelling for iot technologies: Applications and challenges,” *IEEE Access*, vol. 10, pp. 24 095–24 131, 2022.
- [23] S. J. Danbatta and A. Varol, “Comparison of zigbee, z-wave, wi-fi, and bluetooth wireless technologies used in home automation,” in *2019 7th International Symposium on Digital Forensics and Security (ISDFS)*. IEEE, 2019, pp. 1–5.
- [24] G. Lopez, J. Matanza, D. De La Vega, M. Castro, A. Arrinda, J. I. Moreno, and A. Sendin, “The role of power line communications in the smart grid revisited: Applications, challenges, and research initiatives,” *IEEE access*, vol. 7, pp. 117 346–117 368, 2019.
- [25] E. Kabalci and Y. Kabalci, *Smart grids and their communication systems*. Springer, 2019, no. 1.
- [26] J. Slacik, P. Mlynek, M. Rusz, P. Musil, L. Benesl, and M. Ptacek, “Broadband power line communication for integration of energy sensors within a smart city ecosystem,” *Sensors*, vol. 21, no. 10, p. 3402, 2021.
- [27] W. Ejaz, A. Anpalagan, W. Ejaz, and A. Anpalagan, “Internet of things for smart cities: overview and key challenges,” *Internet of Things for Smart Cities: Technologies, Big Data and Security*, pp. 1–15, 2019.
- [28] R. Dotihal, A. Sopori, A. Muku, N. Deochake, and D. Varpe, “Smart homes using alexa and power line communication in iot,” in *International Conference on Computer*

- Networks and Communication Technologies: ICCNCT 2018*. Springer, 2019, pp. 241–248.
- [29] O. A. Gonzalez, J. Urminsky, M. Calvo, and L. De Haro, “Performance analysis of hybrid broadband access technologies using plc and wi-fi,” in *2005 International Conference on Wireless Networks, Communications and Mobile Computing*, vol. 1. IEEE, 2005, pp. 564–569.
- [30] M. Shwehdi and A. Khan, “A power line data communication interface using spread spectrum technology in home automation,” *IEEE Transactions on Power Delivery*, vol. 11, no. 3, pp. 1232–1237, 1996.
- [31] T. Zahariadis, K. Pramataris, and N. Zervos, “A comparison of competing broadband in-home technologies,” *Electronics & communication engineering journal*, vol. 14, no. 4, pp. 133–142, 2002.
- [32] S. Du, S. Chen, W. Peng, and B. Zhao, “An improved power line communication system based on fh-ofdm transmission scheme,” in *2022 2nd International Conference on Intelligent Technology and Embedded Systems (ICITES)*. IEEE, 2022, pp. 1–5.
- [33] C. Cano, A. Pittolo, D. Malone, L. Lampe, A. M. Tonello, and A. G. Dabak, “State of the art in power line communications: From the applications to the medium,” *IEEE Journal on Selected Areas in Communications*, vol. 34, no. 7, pp. 1935–1952, 2016.
- [34] E. J. Lima, M. H. S. Bomfim, and M. A. d. M. Mourão, “Polibot–power lines inspection robot,” *Industrial Robot: An International Journal*, vol. 45, no. 1, pp. 98–109, 2018.
- [35] D. Miller, G. Mirzaeva, and G. Goodwin, “Power line communication in emergency power microgrid for mining industry,” in *2020 IEEE Industry Applications Society Annual Meeting*, 2020, pp. 1–6.

- [36] W. Ding, F. Yang, H. Yang, J. Wang, X. Wang, X. Zhang, and J. Song, "A hybrid power line and visible light communication system for indoor hospital applications," *Computers in industry*, vol. 68, pp. 170–178, 2015.
- [37] J. Song, W. Ding, F. Yang, H. Yang, J. Wang, X. Wang, and X. Zhang, "Indoor hospital communication systems: An integrated solution based on power line and visible light communication," in *2014 IEEE Faible Tension Faible Consommation*. IEEE, 2014, pp. 1–6.
- [38] L. Zhang, X. Liu, and D. Xu, "A novel security monitoring system of coal mine based on power line communication dynamic routing technology," in *2014 IEEE Industry Application Society Annual Meeting*. IEEE, 2014, pp. 1–6.
- [39] L. G. da Silva Costa, A. C. M. de Queiroz, B. Adebisi, V. L. R. da Costa, and M. V. Ribeiro, "Coupling for power line communications: A survey," *Journal of Communication and Information Systems*, vol. 32, no. 1, 2017.
- [40] C. E. G. Moreta, M. R. C. Acosta, and I. Koo, "Prediction of digital terrestrial television coverage using machine learning regression," *IEEE Transactions on Broadcasting*, vol. 65, no. 4, pp. 702–712, 2019.
- [41] C. E. Garcia, M. R. Camana, and I. Koo, "Ensemble learning aided qpso-based framework for secrecy energy efficiency in fd cr-noma systems," *IEEE Transactions on Green Communications and Networking*, 2022.
- [42] M. Khan and S. Noor, "Performance analysis of regression-machine learning algorithms for predication of runoff time. agrotechnology 08 (01): 1–12," 2019.
- [43] Y. Zhang, J. Wen, G. Yang, Z. He, and J. Wang, "Path loss prediction based on machine

- learning: Principle, method, and data expansion,” *Applied Sciences*, vol. 9, no. 9, p. 1908, 2019.
- [44] C. E. Garcia and I. Koo, “Coverage prediction and rem construction for 5g networks in band n78,” in *2023 15th International Conference on Computer and Automation Engineering (ICCAE)*. IEEE, 2023, pp. 125–129.
- [45] Y. Zhao, J. H. Reed, S. Mao, and K. K. Bae, “Overhead analysis for radio environment mapenabled cognitive radio networks,” in *2006 1st IEEE Workshop on Networking Technologies for Software Defined Radio Networks*. IEEE, 2006, pp. 18–25.
- [46] A. Achtzehn, J. Riihijärvi, I. A. Barriúa Castillo, M. Petrova, and P. Mähönen, “Crowdrem: Harnessing the power of the mobile crowd for flexible wireless network monitoring,” in *Proceedings of the 16th International Workshop on Mobile Computing Systems and Applications*, 2015, pp. 63–68.
- [47] J. Wang, N. Tan, J. Luo, and S. J. Pan, “Woloc: Wifi-only outdoor localization using crowdsensed hotspot labels,” in *IEEE INFOCOM 2017-IEEE Conference on Computer Communications*. IEEE, 2017, pp. 1–9.
- [48] S. Debroy, S. Bhattacharjee, and M. Chatterjee, “Spectrum map and its application in resource management in cognitive radio networks,” *IEEE Transactions on Cognitive Communications and Networking*, vol. 1, no. 4, pp. 406–419, 2015.
- [49] V. Chowdappa, C. Botella, J. Samper-Zapater, and R. Martinez, “Distributed radio map reconstruction for 5 g automotive, iee intell. transp. syst. mag. 10 (2)(2018) 36–49,” 2018.
- [50] S. Roger, C. Botella, J. J. Pérez-Solano, and J. Perez, “Application of radio environment

- map reconstruction techniques to platoon-based cellular v2x communications,” *Sensors*, vol. 20, no. 9, p. 2440, 2020.
- [51] O. O. Erunkulu, A. M. Zungeru, C. K. Lebekwe, and J. M. Chuma, “Cellular communications coverage prediction techniques: A survey and comparison,” *IEEE Access*, vol. 8, pp. 113 052–113 077, 2020.
- [52] P. Maiti and D. Mitra, “Complexity reduction of ordinary kriging algorithm for 3d rem design,” *Physical Communication*, vol. 55, p. 101912, 2022.
- [53] M. Pesko, T. Javornik, A. Košir, M. Štular, and M. Mohorčič, “Radio environment maps: The survey of construction methods.” *KSII Transactions on Internet & Information Systems*, vol. 8, no. 11, 2014.
- [54] Z. Han, J. Liao, Q. Qi, H. Sun, J. Wang *et al.*, “Radio environment map construction by kriging algorithm based on mobile crowd sensing,” *Wireless Communications and Mobile Computing*, vol. 2019, 2019.
- [55] P. Maiti and D. Mitra, “Ordinary kriging interpolation for indoor 3d rem,” *Journal of Ambient Intelligence and Humanized Computing*, vol. 14, no. 10, pp. 13 285–13 299, 2023.
- [56] D. Shepard, “A two-dimensional interpolation function for irregularly-spaced data,” in *Proceedings of the 1968 23rd ACM national conference*, 1968, pp. 517–524.
- [57] D. Plets, W. Joseph, K. Vanhecke, E. Tanghe, and L. Martens, “Coverage prediction and optimization algorithms for indoor environments,” *EURASIP Journal on Wireless Communications and Networking*, vol. 2012, no. 1, pp. 1–23, 2012.
- [58] P. Sruthi and K. Sahadevaiah, “A novel efficient heuristic based localization paradigm

- in wireless sensor network,” *Wireless Personal Communications*, vol. 127, no. 1, pp. 63–83, 2022.
- [59] R. He, Y. Gong, W. Bai, Y. Li, and X. Wang, “Random forests based path loss prediction in mobile communication systems,” in *2020 IEEE 6th International Conference on Computer and Communications (ICCC)*. IEEE, 2020, pp. 1246–1250.
- [60] U. Masood, H. Farooq, and A. Imran, “A machine learning based 3d propagation model for intelligent future cellular networks,” in *2019 IEEE Global Communications Conference (GLOBECOM)*. IEEE, 2019, pp. 1–6.
- [61] H. Singh, S. Gupta, C. Dhawan, and A. Mishra, “Path loss prediction in smart campus environment: Machine learning-based approaches,” in *2020 IEEE 91st Vehicular Technology Conference (VTC2020-Spring)*. IEEE, 2020, pp. 1–5.
- [62] S. Ojo, A. Imoize, and D. Alienyi, “Radial basis function neural network path loss prediction model for lte networks in multitransmitter signal propagation environments,” *International Journal of Communication Systems*, vol. 34, no. 3, p. e4680, 2021.
- [63] M. Sousa, A. Alves, P. Vieira, M. P. Queluz, and A. Rodrigues, “Analysis and optimization of 5g coverage predictions using a beamforming antenna model and real drive test measurements,” *IEEE Access*, vol. 9, pp. 101 787–101 808, 2021.
- [64] H.-S. Jo, C. Park, E. Lee, H. K. Choi, and J. Park, “Path loss prediction based on machine learning techniques: Principal component analysis, artificial neural network, and gaussian process,” *Sensors*, vol. 20, no. 7, p. 1927, 2020.
- [65] N. Moraitis, L. Tsipi, D. Vouyioukas, A. Gkioni, and S. Louvros, “Performance evaluation of machine learning methods for path loss prediction in rural environment at 3.7 ghz,” *Wireless Networks*, vol. 27, no. 6, pp. 4169–4188, 2021.

- [66] C. E. GARCÍA and I. Koo, “Extremely randomized trees regressor scheme for mobile network coverage prediction and rem construction,” *IEEE Access*, 2023.